EXPERIMENTAL AND STATISTICAL STUDY ON

THE PERMANENT DEFORMATION BEHAVIOR OF

GRANULAR SOIL

By

SPANDANA ANNAMRAJU

Bachelor of Technology in Civil Engineering

Gayatri Vidya Parishad College of Engineering, JNTU K

Visakhapatnam, Andhra Pradesh

2011

Submitted to the Faculty of the
Graduate College of the
Oklahoma State University in
partial fulfillment of

the requirements for the
Degree of MASTER OF
SCIENCE December,
2014

EXPERIMENTAL AND STATISTICAL STUDY ON THE PERMANENT
DEFORMATION BEHAVIOR OF GRANULAR SOIL

Thesis Approved:

Dr. Xiaoming Yang

Thesis Adviser

Dr. Rifat Bulut

Dr. Tyler Ley

ACKNOWLEDGEMENTS

First and foremost, I would like to use this opportunity to express my gratitude and indebtedness to my advisor, Dr. Xiaoming Yang who has encouraged me throughout my Master's program. He helped me all the way with his support, knowledge and patience and was always available for discussions. One simply couldn't wish for a better and friendlier guide. I would like to express my grateful acknowledgment to Dr. Rifat Bulut and Dr. Tyler Ley for agreeing to be my committee members. I would like to thank Mr. David Porter who helped me throughout this thesis in using the lab equipment.

I take this opportunity to specially thank my friend Sruthi Mantri who has always been there in my low times and encouraged me and made this possible. I would like to extend my thanks to my friends Anjana and Krishen and my cousins Pushya and Rajesh Mantri for their support and encouragement throughout my Master's program. I would like to thank my colleagues Roman Poudyal and Siddharth Tithe who has supported me and helped me all the time. I would like to extend my thanks to my loving parents and my brother who really supported me and understood me from a long distance. I thank the Almighty for being there with me all the time and showering his blessings

Name: SPANDANA ANNAMRAJU

Date of Degree: DECEMBER, 2014

Title of Study: EXPERIMENTAL AND STATISTICAL STUDY ON THE
PERMANENT DEFORMATION BEHAVIOR OF GRANULAR SOIL

Major Field: CIVIL AND ENVIRONMENTAL ENGINEERING

Abstract:

The primary objective of this research is to study the permanent deformation behavior of a granular soil. The permanent deformation behavior of granular soils is strongly related to the rut depth development in flexible pavements. Repeated Load Triaxial (RLT) tests have the ability to simulate the cyclic pavement loading on the granular materials. However, no test standard is currently available. A comprehensive laboratory experimental work was carried out in this study on a poorly graded sand. The experimental work included resilient modulus tests and both single-stage and multi-stage RLT tests. The analysis of the permanent deformation of the sand was carried out by statistical analysis. A regression model was developed to describe the permanent strain accumulation with the number of load cycles at different stress conditions. A test procedure is proposed to for determining the material parameters for the proposed model.

TABLE OF CONTENTS

Chapter   Page

LIST OF TABLES

LIST OF FIGURES

CHAPTER I

INTRODUCTION

1.1 Problem Statement

The performance of flexible pavement structures largely depends on the permanent deformation behavior of unbound materials in the base, subbase, and subgrade layers under repeated loads. The development of permanent strain under a large number of repeated loads is a very special and complicated behavior of granular soils. It is related to the soil type, compaction density, moisture content, and most importantly, the stress condition. In the current AASHTO pavement design standard, the permanent deformation model of unbound granular soils is over-simplified, and it is insensitive to the stress condition.

In order to improve the design method of for flexible pavements, Strategic Highway Research Program (SHRP), Federal Highway Administration (FHWA), and National Cooperative Highway Research Program (NCHRP) suggested further research on the permanent deformation properties of the granular materials (Austin, 2002). The best way to characterize the permanent deformation behavior of granular soils is to conduct permanent deformation test on the soil using the repeated load triaxial (RLT) device. Permanent deformation tests include parameters like confining pressure, deviator stress and the number of loading cycles. In the past, many researchers have performed the permanent deformation tests granular soils and proposed different models to describe the test result. However, there is still a lack of basic agreement on how to run

a permanent deformation test and which model should be used to describe the permanent deformation behavior of granular soils.

1.2 Research Objectives

The objectives of this study are

1. To characterize the permanent deformational behavior of a poorly graded sand using RLT test.

2. To develop a relationship between permanent strain and and load cycles N considering the effect of confining and deviatoric stress levels.

3. To propose a permanent deformation test procedure to calibrate the parameters in the proposed model

1.3 Scope of this study

A poorly graded silica sand was used to accomplish the objectives of this research. Physical property tests like sieve analysis, minimum and maximum index density tests, direct shear tests, and resilient modulus tests were conducted on the sand. Repeated loa triaxial tests was performed to characterize the behavior of the sand under a large number of repeated load. Two types of repeated loading tests were conducted in this study: single-stage tests and multi-stage tests. Since no standard procedure is available, a range of confining pressures and deviator stresses were selected in the permanent deformation tests. After the analyses of the results, a permanent deformation model was developed and a standard test procedure was suggested for further research.

1.4 Organization of the Document

The thesis is organized in five chapters including the introductory chapter.

Chapter 2 presents the previous literature and studies of several researchers related to resilient modulus and permanent deformation.

Chapter 3 describes the experimental testing program for the determination of permanent strain. It also includes the physical property tests on the sand.

Chapter 4 summarizes all the results and analyzes the results to determine the behavior of the soils.

Chapter 5 attains conclusions and some further research recommendations.

CHAPTER II

LITERATURE REVIEW

2.1 Introduction

The overall behavior of a pavement largely depends on the foundation layers, i.e; subgrade, subbase, and base course. The deformation of the pavements was studied focusing on the sub grade layer. Sub grade plays the main role as a load bearing layer. The resilient and permanent deformations were investigated in the sub grade layers with the effect of stresses and repeated loading. Several factors affecting the resilient modulus and permanent deformation behavior and numerical models for predicting the resilient modulus and permanent deformation are discussed.

The stresses on the pavement due to wheel load is related to principal stress rotation theory. An elemental cube is considered with normal and shear stresses acting on it. These stresses can be calculated with any orientation if the principal stresses are known. The simulation of shear stress is difficult in the laboratory. However, the resulting stresses are represented as normal stresses which are shown in Fig. 2.1. These are the principal stresses σ_x and σ_y. Figure 2.2 explains the wheel load effect on the pavement. A contact stress will occur when a load is applied.
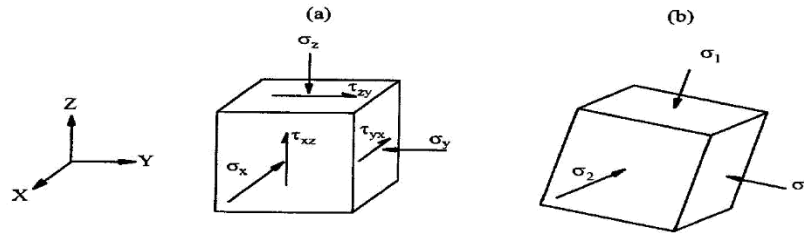
Figure 2.1. Stress components acting on an element (Lekarp 97)
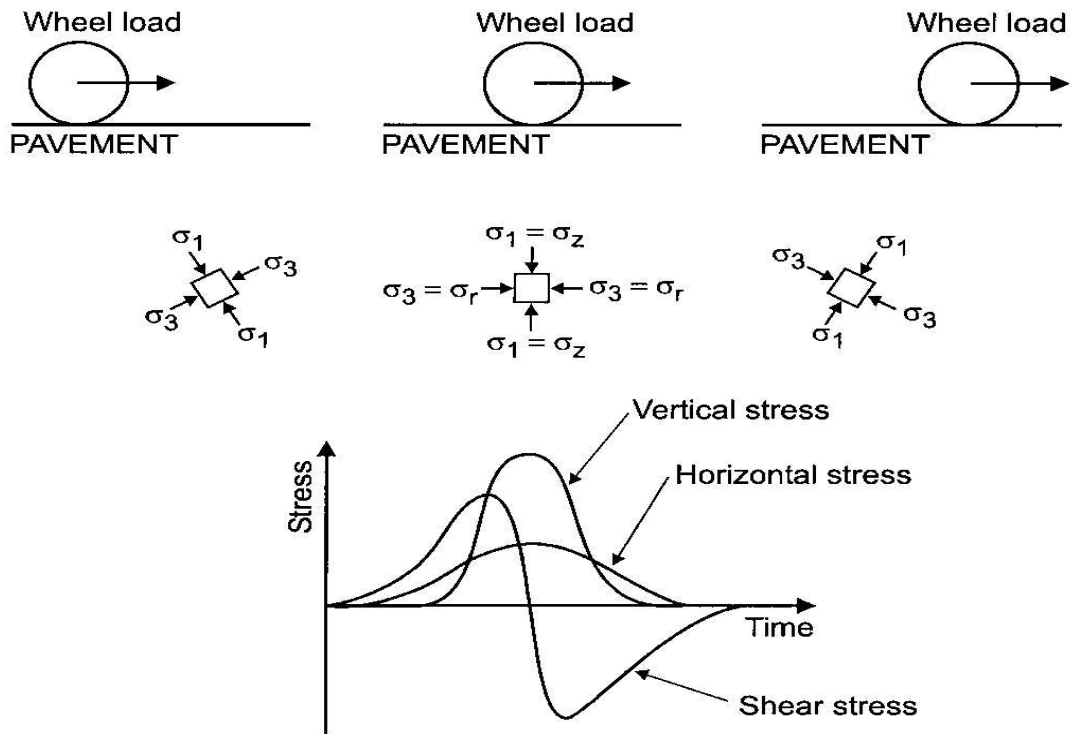
Figure 2.2. Stresses beneath rolling wheel load (Lekarp et al. 2000)

Stress will remain the same as long the load is completely in contact with the soil. Some cases where there are unequal loads on the surface, stresses vary accordingly. In case of a wheel load, the load applied is not evenly applied throughout the soil. There will be unequal load points at different locations depending on the factors like depth from the surface, distance from the applied loading and soil type.

Soils, in general exhibit elastic-plastic behavior. An elastic deformation is a type in which the material recovers its antecedent position. A plastic deformation is another type of deformation in which the material undergoes a permanent deformation. The purpose of this study is to investigate the deformation behavior in sub grade soils in the context of resilient modulus and permanent deformation testing.

2.2 Resilient Modulus and Permanent Deformation

Resilient modulus is defined as the ratio of axial deviator stress to resilient strain. This resilient strain is the recoverable axial strain. Resilient modulus is presented in the equation 2.1

$$=$$

Equation 2.1

Where $=$ axial deviator stress

$=$ axial recoverable strain

Permanent deformation is a result of repeated loading from traffic resulting in the amalgamation to form plastic deformation. This type of deformation occurs when repeated loading is applied.
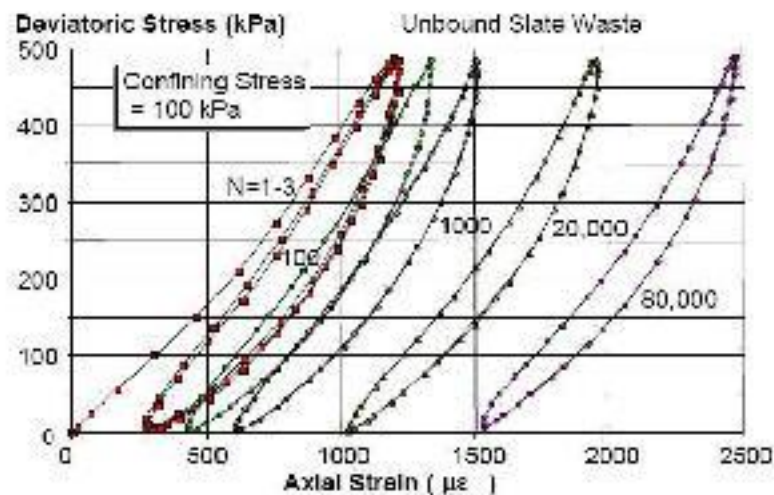
Figure 2.3. RLT test for unbound slate waste (Dawson and Nunes, 1994)

Dawson and Nunes performed repeated load triaxial tests on unbound slate waste with a confining pressure of 100kPa. They plotted a graph with deviator stress versus strain and observed a hysteresis loop. Figure 2.4 represents the hysteresis loop pattern with 80,000 loading cycles. As the number of cycles increase, the hysteresis loop becomes narrower and a single loop cannot be observed. This shows a marked decrease in permanent deformation. This case happens at lower stress levels. Depending on the stress levels, permanent deformation may increase, decrease or remain constant and may fail with increasing number of loading cycles. Figure 2.4 represents stress strain graph with permanent and resilient strains during one load cycle.
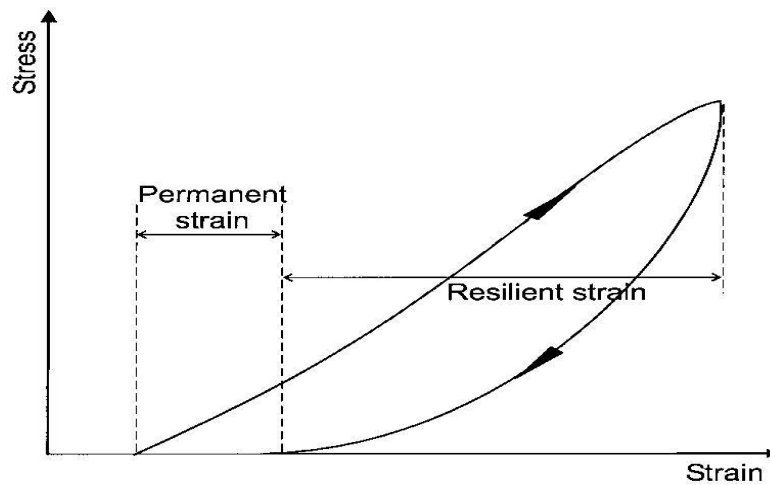
Figure 2.4. Strains in granular materials during one cycle of load application

(Lekarp et al. 2000)

2.3 Previous Research on Repeated Load Triaxial (RLT) Tests

Several researchers performed repeated triaxial loading tests, resilient modulus tests and permanent deformation tests to investigate the permanent strain and deformation studies of the material which are detailed in Table 2.1. The confining pressure (σ_3) and the deviator stress (σ_d) data was detailed along with the type of material and standard used in the study.

Table 2.1 Repeated Loading Test Data

Reference	Pre conditioning	Loading								Materi
Chen et al. (2013)	1000 cycles at cyclic and confining stresses of 93 and 103.4 kPa	Stage	Test 1		Test 2		Test 3		N	Geogri reinforc granula base materia
			σ_3 (kPa)	σ_d (kPa)	σ_3 (kPa)	σ_d (kPa)	σ_3 (kPa)	σ_d (kPa)		
		1	72	43	145	136	198	210	10000	
		2	72	91	145	183	198	276	10000	
		3	72	120	145	229	198	328	10000	
		4	72	155	145	274	198	397	10000	
		5	72	183	145	319	198	473	10000	
		6	72	195	145	350	198	510	10000	
Cerni et al. (2011)	-	Stage	σ_3 (kPa)		σ_d (kPa)		N			Granula materia
		1	20		10		10000			
		2	50		25		10000			
		3	70		35		10000			
		4	150		75		10000			
Mengelt et al. (2006)	1000 cycles	Stage	σ_3 (kPa)		σ_d (kPa)		N			Coarse and fin graine soil
		1	21		25		1500			
		2	34		50		1500			
		3	69		75		1500			
		4	103		100		1500			

Table 2.1 Repeated Loading Test Data (Cont'd)

Reference	Pre conditioning	Loading							Mater
Kumar et al. (2006)	No	Stage	σ_3 (kPa)		σ_d (kPa)		N		Sub ba mater
		1	40		125		10000		
		2	70		95		10000		
		3	100		65		10000		
Guimaraes and Motta (2008)	No	Stage	σ_3 (kPa)		σ_d (kPa)		N		Lateri soils
		Test 1	105		105		161312		
		Test 14	105		157,5		231453		
		Test 2	105		210		245252		
		Test 3	105		315		257200		
Li (2013)	50 cycles at 103.4 kPa confining pressure	Stage	ISU 100 K TEST		ISU 100 K TEST		NCHRP report 598		Sub ba mater
			σ_d (kPa)	N	σ_d (kPa)	N	σ_d (kPa)	N	
		1	34.5	25,000	34.5	250	34.5	1000	
		2	34.5	25,000	34.5	250	34.5	1000	
		3	34.5	25,000	34.5	250	172.4	1000	
		4	34.5	25,000	34.5	250	310.3	1000	
		5					448.2	1000	
		6					586.1	1000	
		7					724	1000	
		8					861.9	1000	
		9					998.9	1000	
		10					1137.7	1000	

Table 2.1 Repeated Loading Test Data (Cont'd)

Reference	Pre conditioning	Loading								Materi
Rahman et al. (2014)	-	Stage	σ_3 (kPa)		σ_d (kPa)		N			Geogri
		1	50		150		10000			reinforc
		2	50		250		10000			C&D
		3	50		300		10000			materi
Austin (2009)	1000 cycles at 15 psi confining pressure and 14 psi axial stress	Stage (Limes tone)	Test 1		Test 2		Test 3		N	Base cou materi
			σ_3 (kPa)	σ_d (kPa)	σ_3 (kPa)	σ_d (kPa)	σ_3 (kPa)	σ_d (kPa)		
		1	4.3	3.8	7.4	8.5	12.6	18.0	10000	
		2	6.1	9.1	10.4	17.5	18.0	34.3	10000	
		3	9.0	18.0	12.8	24.9	21.3	44.0	10000	
		4	14.5	34.5	19.3	44.4	24.9	55.0	10000	
		5	20.1	51.3	27.8	70.0	33.6	80.1	10000	
		6	21.3	54.8	31.4	81.4	34.0	82.6	10000	
		Stage (Sands tone)	Test 1		Test 2		Test 3		N	
			σ_3 (kPa)	σ_d (kPa)	σ_3 (kPa)	σ_d (kPa)	σ_3 (kPa)	σ_d (kPa)		
		1	3.2	3.7	12.5	18.0	15.9	17.6	10000	
		2	6.1	8.9	15.5	27.0	21.4	33.9	10000	
		3	7.7	14.1	17.9	34.0	24.7	43.8	10000	
		4	14.5	34.3	23.3	50.2	29.5	58.2	10000	
		5	16.6	40.7	27.3	62.4	30.9	62.6	10000	
		6	20.2	51.3	28.3	65.4	31.8	65.2	10000	

Table 2.1 represents the confining pressure, deviator stress and number of loading cycles in each stage of the RLT tests performed several researchers. Chen et al. (2013) performed a shakedown analysis of geogrid-reinforced granular base material. A shakedown behavior was analyzed to evaluate the factors affecting the shakedown stress limits. He concluded that inclusion of the geogrid-reinforcement reduced the accumulation of the permanent deformation.

Cerni et al. (2011) performed repeated triaxial loading tests on two unbound granular materials with four loading stages for road subbase layers. The permanent deformation behavior was analyzed based on the shakedown approach. The frictional behavior of the mixture was able to undergo high stress levels before the accumulation of plastic strain. A mathematical model was developed to predict the behavior of permanent deformation.

Mengelt et al. (2006) performed resilient modulus and permanent deformation tests in a geocell. The preconditioning and loading stages were expressed in Table 2.1. Resilient modulus was conducted on two coarse-grained soil and a fine-grained soil. Resilient modulus increased by 1.4-3.2% when the infill was coarse-grained material and increased by 16.5-17.9%.

Different subbase materials were compared using static and cyclic triaxial tests by Kumar et al. (2006). He observed that a river bed material has a good CBR, high resilient modulus and low permanent strain when compared to other materials used in this study. A k-θ model was developed from this study.

Three lateritic soils were tested for permanent and resilient deformation using repeated triaxial tests with number of cycles greater than 100,000. Guimaraes and Motta (2008) studied the occurrence of plastic shakedown or material shakedown was investigated. Tests 1 and 14 belong to a single lateritic soil with different deviator stress. All the tests were highly influenced by the stress state and moisture content of the test specimens.

Rahman et al. (2014) used construction and demolition materials for testing. The Mr value increased by 24% in biaxial and 34% in triaxial recycled concrete aggregate (RCA). The results indicate that with increasing deviator stress and a constant confining pressure, permanent strain have increased.

Li (2013) performed studies using resilient and permanent deformation tests. Three methods of tests were used in loading stage named ISU 100k test, ISU 1k test and NCHRP 598. ISU 100k tests have the loading sequences which produce large permanent deformation as there are high stresses. An axial strain of 5% was observed in ISU 100k and ISU 1k tests. NCHRP 598 consists of one preconditioning sequence and 10 loading sequences. It was observed that resilient modulus values are not increasing with the number of load applications.

Sandstone, limestone and granite were tested by Austin (2009). The unbound materials were examined under different loading conditions. Single stage and multi stage tests were conducted on all the samples. The results conclude that sandstone experienced largest permanent and resilient strain in both single stage and multi stage tests. Granite has the lowest permanent and resilient strain when compared to limestone. The resilient and permanent strains are stress dependent. However, the resilient behavior is distinct from the permanent strain.

2.4 Factors affecting Permanent Deformation Behavior

When compared to the resilient response, less research have been done on the permanent deformation, especially in case of granular materials. Research on permanent deformation is a destructive and time-consuming process. The permanent deformation behavior of soils is complicated. Lekarp et al. 2000 discussed the factors affecting the permanent deformation behavior in detail. According to Lekarp et al. 2000, several factors affect the deformation behavior which is listed below.

1. Applied stress

   The axial permanent strain is directly proportional to deviator stress and inversely proportional to confining pressure. The applied stress level has the ability to resist the permanent deformation.

2. Number of loading cycles

   Permanent deformation is accumulation of strain gradually with each load repetition. Hence, number of loading cycles plays a major role in the analysis of long-term permanent strain behavior.

3. Density

   The effect of density is important and it is related to the degree of compaction. The plastic strain decreases with increase in density for angular aggregates. With increased density, strain decreases for rounded aggregates.

4. Stress history

   The permanent deformation behavior, number of loading cycles and stress history are directly related to each other.

2.5 Models for predicting permanent deformation behavior

A complex strain behavior occurs while predicting the permanent deformation. Several researchers attempted several procedures to find the magnitude of the permanent deformation. Factors which affect the permanent strain like number of loading cycles, stress conditions, deviator stress, static strength and confining pressure are used to develop different modeling techniques. Long-term behaviors of granular materials were used in establishing constitutive relationships which are discussed below. Lekarp et al. 2000 discussed many models developed by several researchers which are detailed in Table 2.2. Several other researcher's models are also shown in the table.
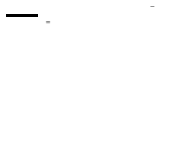
Table 2.2 Models for predicting permanent strain
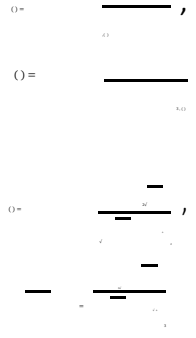
Numerical Model	Reference	Parameters	Material
	Veverka (1979)	= accumulated permanent axial strain after given number of load cycles = resilient strain a, b = regression parameters	Sand-gravel mixture
	Jouve et al. (1987)	, = bulk and shear moduli with respect to permanent deformation A_2, A_3, D_2, D_4 = parameters that are functions of stress ratio q/p , = permanent volumetric and shear strain for N>100	Unbound base course material
	Khedr (1985)	A, B = regression parameters N = number of loading cycles	Granular crushed limestone
	Barksdale (1972)		Soil aggregate mixture
	Sweere (1990)	a, b, c = regression parameters	Crushed stone
	Wolff and Visser (1994)	N = number of loading cycles	Crushed stone, natural gravel

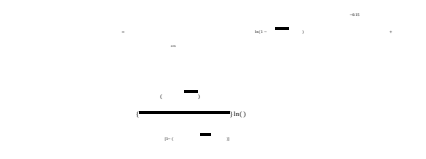**Table 2.2 Models for predicting permanent strain (Cont'd)**
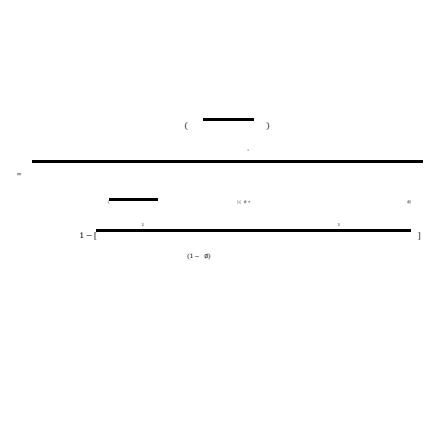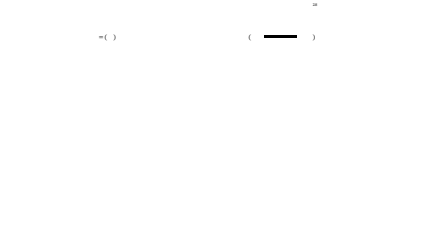
Numerical Model	Reference	Parameters	Material
	Paute et al. (1996)	permanent strain after 100 cycles	Silty sand
	Barksdale (1972)	C = apparent cohesion = confining pressure = ratio of the measured strength to ultimate hyperbolic strength Ø = angle of internal friction	Limestone material
	Lentz and Baladi (1981)	q = deviator stress S = static strength = confining pressure	Cohesionless subgrade material
	Lashine et al. (1971)		Silty clay
	Pappin (1979)	= shape factor = modified deviator stress = √2/3 q = modified mean normal stress = √3 p	Crushed rock
PD = A (-1)	Theyse (1997)	PD = Permanent Deformation (mm) = vertical stress on top of pavement foundation (kPa) A, B = regression constants	Uncrushed gravel base

Table 2.2 Models for predicting permanent strain (Cont'd)

Numerical Model	Reference	Parameters	Material
PD = (-1)	Theyse (1997)	c = intersect of straight line relationship A and N s = slope	Uncrushed gravel base
	Wu and Chen (1997)	PD(N) = permanent deformation for pavement layer/sublayer after N cycles = reference cycles PD( ) = ABACUS calculated permanent deformation after cycles	Cement and lime treated soil
$= \beta_{s1} \, k_{s1} (\quad)$	MEPDG Model	= permanent strain ε_o = Intercept ε_r = Resilient strain k_{s1}, β_{s1} = calibration coefficients	HMA mixtures, unbound materials

CHAPTER III

EXPERIMENTAL TESTING PROGRAM

3.1 Soil Properties Tests

Several laboratory tests were performed to screen the physical properties of the silica sand. ASTM C136-06 and ASTM D422 were the standard testing procedures used for the sieve analysis of fine and coarse aggregates. Minimum and maximum Index density tests were performed according to ASTM D4254 and ASTM D4253 respectively. Direct shear tests were performed based on ASTM D3080. Finally, resilient modulus tests were performed based on AASHTO T 307.

3.2 Repeatability Tests

The repeatability of the permanent deformation tests was first investigated to evaluate the reliability of equipment. Two groups of permanent deformation tests were conducted for this purpose. First, seven repeatability permanent deformation tests were conducted at a confining pressure of 5 psi and a deviator stress of 15 psi with 10,000 load repetitions. No preconditioning was done in this group of tests. Second, another seven permanent deformation tests were conducted at the same stress condition and load repetition but with a preconditioning stage.

Table 3.1 Loading and preconditioning stages

Stage	Confining Pressure (psi)	Deviator Stress (psi)	Number of Load Applications
Preconditioning	15	15	1,000
Loading	5	15	10,000

3.3 Permanent Deformation Tests

Permanent deformation tests were performed to determine the permanent strain of the unbound granular soil. Single-stage and multi-stage tests were performed in the permanent deformation tests.

Single-stage tests were performed to determine the permanent deformation with different confining pressures, deviator stress and number of load applications. Twenty one different tests were performed which consist constant confining pressures of 5 psi, 10 psi, 15 psi and 20 psi. The details of the single stage permanent deformation tests can be observed in Table 3.2. Preconditioning stage was not applied in these tests.

Table 3.2 Single-stage tests loading table

No.	Confining Pressure (psi)	Deviator Stress (psi)	Number of Load Applications
Single-Stage Tests			
1	5	5	10,000
2	5	10	10,000
3	5	15	10,000
4	5	20	10,000
5	5	25	Failed
6	10	10	10,000
7	10	20	10,000
8	10	30	10,000
9	10	35	10,000
10	10	40	10,000
11	10	50	Failed
12	15	15	10,000
13	15	30	10,000
14	15	45	10,000
15	15	50	10,000
16	15	60	Failed
17	20	20	10,000
18	20	40	10,000
19	20	60	10,000
20	20	70	10,000
21	20	80	Failed

Table 3.3 Multi-stage tests loading table

No.	Confining Pressure (psi)	Deviator Stress (psi)	Number of Load Applications
Multi-Stage Tests			
1	5	5	2,500
	5	10	2,500
	5	15	2,500
	5	20	2,500
2	10	10	2,500
	10	20	2,500
	10	30	2,500
	10	40	2,500
3	15	15	2,500
	15	30	2,500
	15	45	2,500
	15	60	2,500
4	20	20	2,500
	20	40	2,500
	20	60	2,500
	20	70	2,500

3.3.1 Test Procedure

The amount of soil used for the test was weighed initially. The grease was applied to the apparatus where the latex membrane is associated. Vacuum grease was also applied at the ends of the cylindrical glass chamber to have a smooth contact. The porous stone and latex membrane were placed at the center of the apparatus. The latex membrane was held tight with an O-ring at the groove. The split mold was arranged around the membrane and tightened with the ring. Vacuum was applied so that the membrane is held tight to the split mold without any disturbances. Pour the sand gently in the mold so that the density of the sample is appropriate.

Compact the sample with the vibratory driller which helps to maintain the stiffness and appropriate density of the sample. A compaction plate was placed above the sand to compact.

The position of the vacuum was changed into another valve which connects into the sample. The split mold was carefully removed and the height and diameter of the sample were measured. Arranging the glass chamber around the sample helps prevent the air pressure and rods were arranged prior tightening them. The sample was set up on the resilient modulus apparatus prior arranging the displacement gauge. The confining pressure tube was connected to the pressure valve and the software "rm5" was started.

Figure 3.1 represents the resilient modulus testing machine and the soil sample which was setup for testing. Some samples failed the test if they exceed the strain limit or if large amount of deviator stress is applied. Figure 3.2 represents the schematic diagram of the resilient modulus testing machine. Figure 3.3 represents the sample before the test and when the sample was failed. The load pulse was represented in Figure 3.4. A 0.1 sec load duration and 0.9 sec rest period was observed. A haversine shaped load pulse was formed with a fixed magnitude.
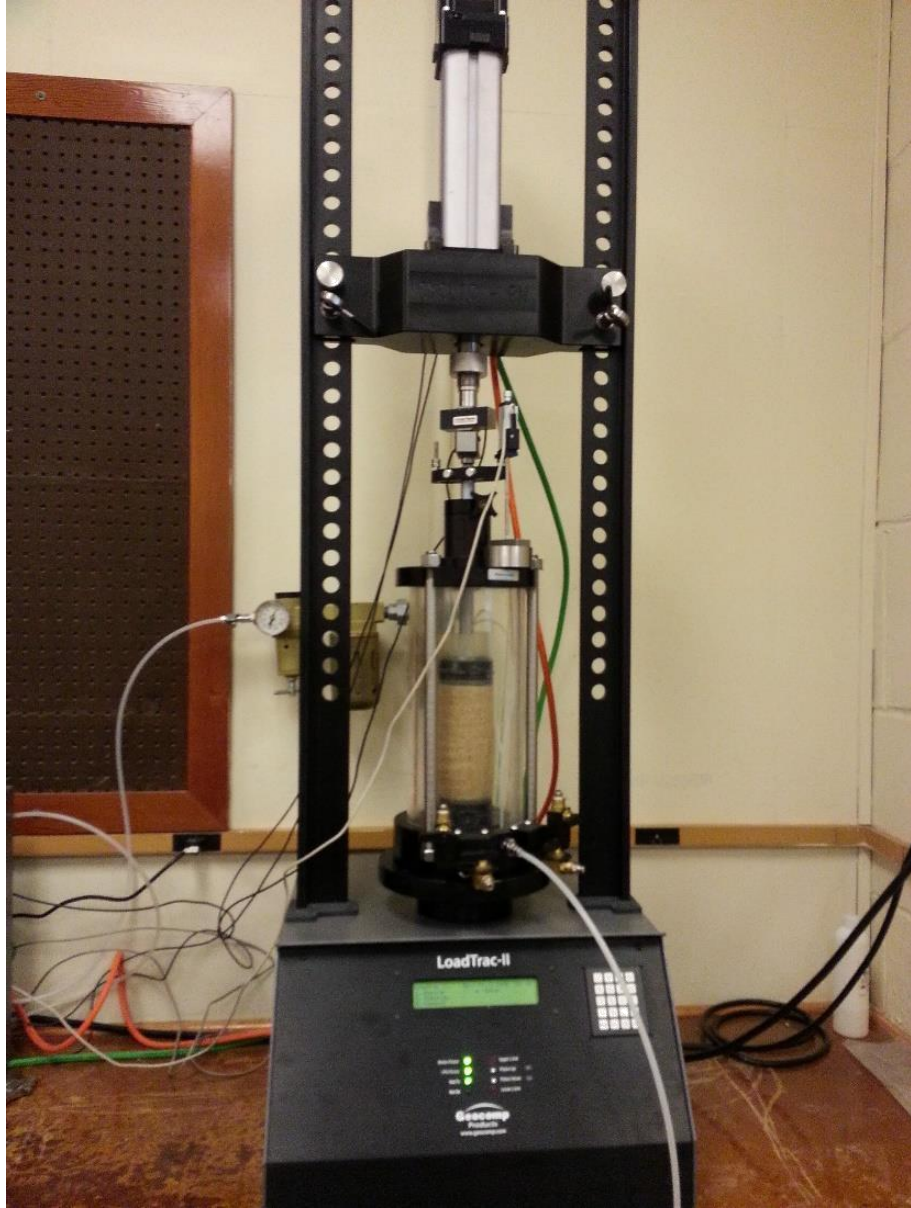
Figure 3.1. Resilient modulus Testing Machine with a soil sample
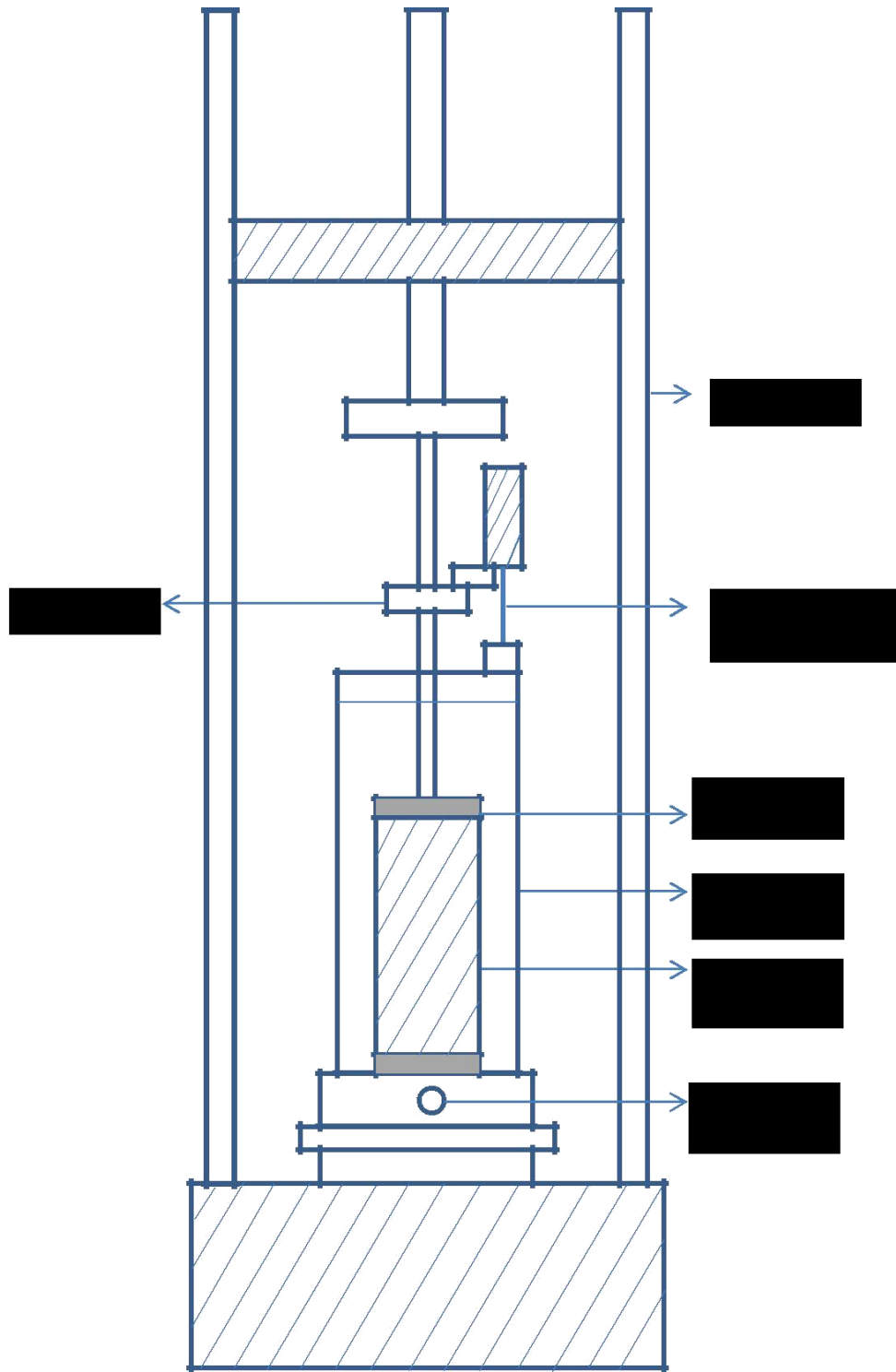
Figure 3.2. Schematic Diagram of the Resilient Modulus Testing Machine

Figure 3.3. Failure of the soil sample in the testing machine
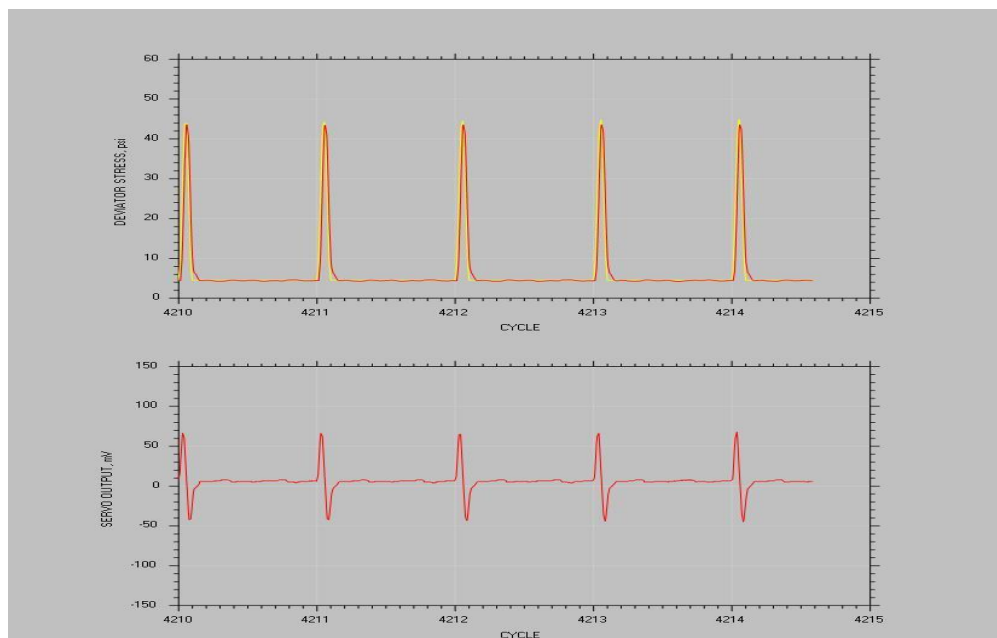
Figure 3.4. Load frequencies while testing

3.3.2 Software Operation

The software was initiated and the specimen and load table data were entered. The load and displacement are zeroed before starting the test using the calibration and system monitor. This was done by adjusting the offset value to zero so that the difference will be minimum. The test was started at this point and the vacuum which is holding the sample can be removed before the rod comes into contact with the sample. The test sequence and graphs can be viewed by test monitor and test graph.

3.3.3 Data Collection

The data and the graphs were obtained after the test is completed. The summary of the data can be obtained from the report. The displacement, pressure and sequence data were obtained from the file. The resilient modulus graphs were also obtained from the report. A table was also given which includes confining pressure, deviator stress and resilient modulus.

CHAPTER IV

RESULTS AND ANALYSES

This chapter analyses the results obtained from the physical property tests and the experimental testing program. The analyses include the characterization of the unbound granular materials under repeated loading.

4.1 Physical Property Test Results

4.1.1 Sieve Analysis

Sieve analysis was performed to determine the gradation of the soil. Figure 4.1 presents the gradation of sand obtained from the test data.
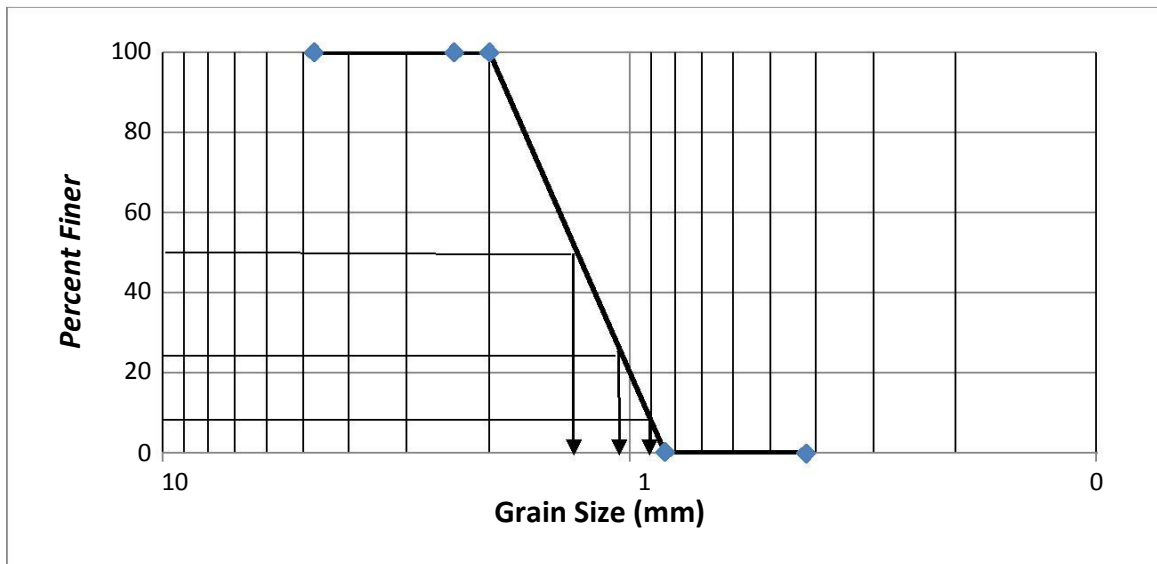
Figure 4.1. Particle size distribution of the granular material

The coefficient of curvature and the coefficient of uniformity of the sand are calculated below.

$D_{10} = 0.91$, $D_{30} = 1.15$, $D_{60} = 1.5$

$$C_c = \frac{^2}{\quad} = 0.97$$

$C_u = \frac{60}{10} = 1.65$

Based on the gradation data and the Unified Soil Classification System (USCS), the sand is classified as a poorly graded sand (SP).

4.1.2 Maximum and Minimum Density

The minimum and maximum density tests were performed with the poorly graded sand. The test was conducted with a mold of 15.2 cm diameter and 15.5 cm height. Three repeated tests were conducted. The test results showed that the average minimum density of the sand is 96.43 lb/ft^3, and the average maximum density of the sand is 107 lb/ft^3.

4.1.3 Direct Shear

Direct shear test was performed at four confining pressures of 5psi, 10psi, 15 psi, and 20psi. The maximum shear stress was calculated at each confining pressure. Figure 4.2 represents the plot from which the friction angle was calculated. The load applied was 24.5lb, 49lb, 73.5lb and 98lb at 5psi, 10psi, 15 psi, and 20psi respectively. The density of the sample was calculated to have an average value of 101.05 lb/ft^3. The density of the sample lies in the range of minimum and maximum densities.
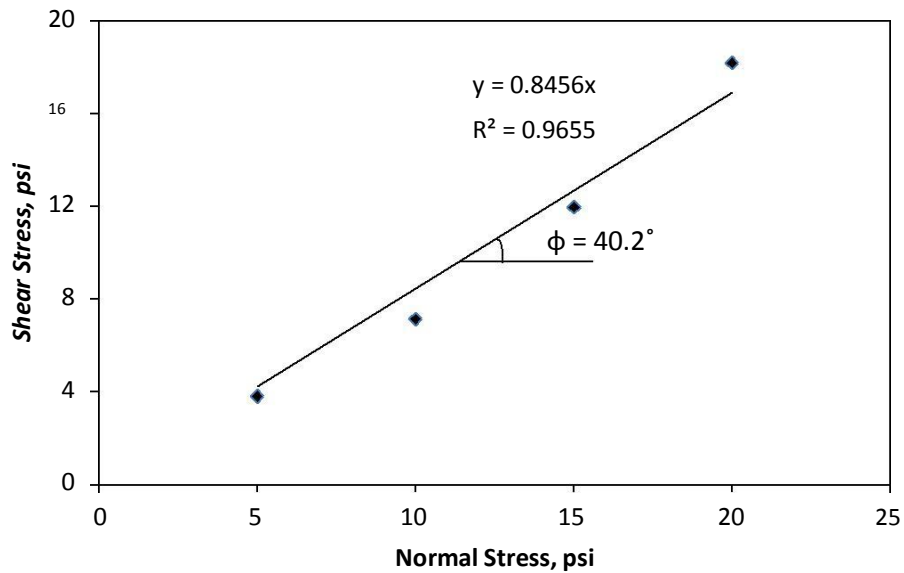
Figure 4.2. Shear stress versus normal stress

4.1.4 Resilient Modulus

Resilient Modulus tests were conducted with confining stresses from 3psi to 20psi. The bulk stress and shear stress were calculated from the data. A multiple linear regression was performed from the bulk stress, shear stress and measured M_r. The details were presented in appendix B. k_1, k_2 and k_3 are the factors calculated from the regression which represent the slope and intercept data. A graph was plotted between resilient modulus (M_r) and bulk stress (θ). It was observed that they have an exponential relationship which is shown in Figure 4.3.
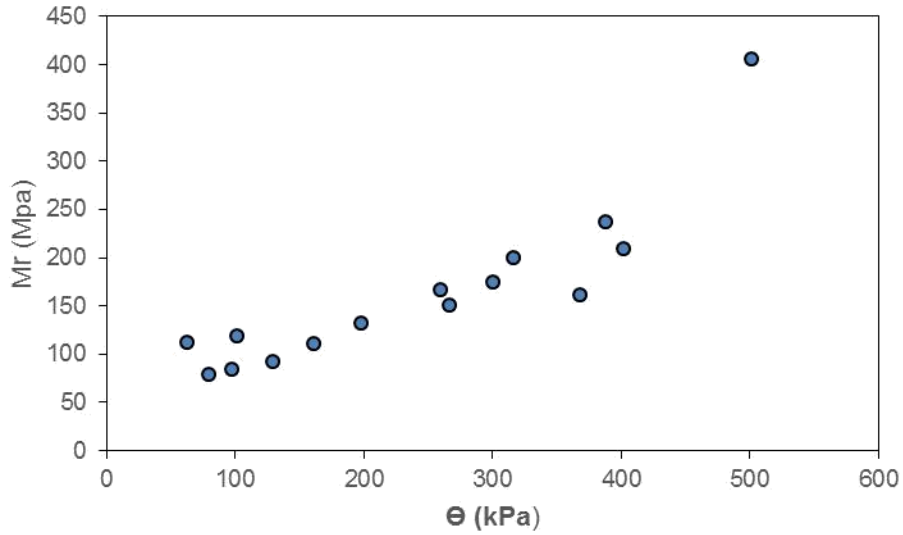
Figure 4.3. Resilient Modulus Graph

4.2 Variability of the permanent deformation tests

Permanent deformation tests were performed using the resilient modulus testing machine. Several confining pressures and deviator stresses were used in this testing procedure. The experimental testing program was explained in detail in Chapter 3. Seven tests were conducted with a constant confining pressure and deviator stress. Table 3.1 shows the details of the loading table. The variability or repeatability of the permanent deformation test was analyzed by repeating the same test with the same input data. The effect of strain on the number of load repetitions was observed.

Figure 4.4 represents the variation of graphs between the permanent strain and number of load repetitions for all the seven tests. The strain ranges from 0.6% to 1%. A test needs to be repeated to make sure the results are correct and can be replicated. The standard deviation of the tests without repeatability was 0.155 and with preconditioning was 0.074.
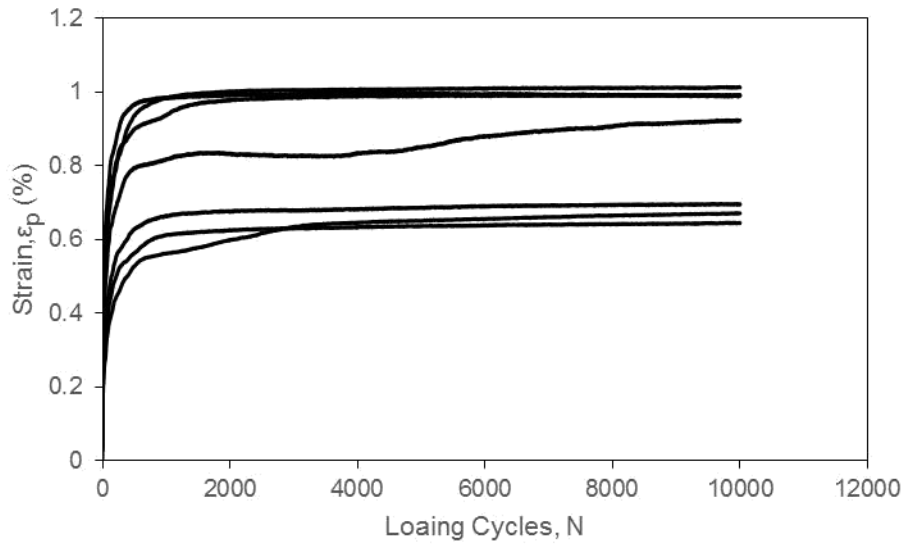
Figure 4.4. Repeatability of the tests without preconditioning
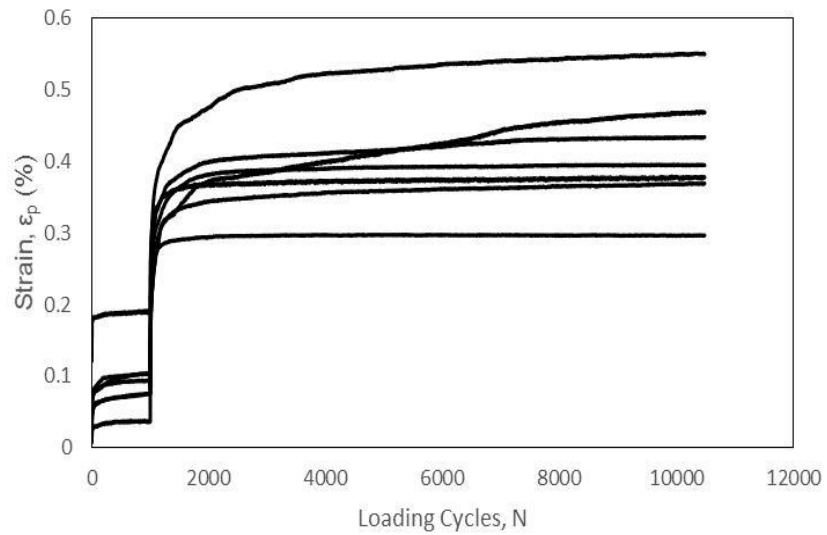
Figure 4.5. Repeatability of the tests with preconditioning

The purpose of the preconditioning stage is to remove the unevenness during sample preparation.

T212he repeatability was observed with the samples which are tested with both preconditioning

and loading stages. Figure 4.4 represents the variability of the strain with preconditioning stage. The strain ranges from 0.3% to 0.6%. It was observed from the Figures 4.4 and 4.5 that the preconditioning have a significant impact on the test repeatability.

4.3 Permanent Deformation Test Results

Permanent deformation tests were conducted and analyzed for the strain and deformation in each case. Single-stage and multi-stage tests were conducted as explained in Chapter 3. The analysis was performed with the test results which is explained below.

4.3.1 Single-Stage RLT Tests

Permanent deformation tests were conducted with different stress conditions. Twenty one different tests were performed to evaluate the stress and strain variations. The effect of confining pressure and deviator stress was studied. The sample failures at a particular deviator stress at each confining pressure were observed. The contact pressure applied at each stress will be 10% of the deviator stress.

Table 3.2 represents the data of the tests conducted with confining pressures of 5 psi, 10 psi, 15 psi, and 20 psi. These tests were conducted with different deviator stresses in each case. Failure of the sample occurred in each case at different deviator stresses. At a confining pressure of 5 psi, the sample failed at a deviator stress of 25 psi. A sample is said to be failed if it exceeds the strain limit and the physical soil sample was observed to be deformed. Permanent deformation is stress-dependent. The stress lies within the range of the deviator stress. The non-correlation of the graphs in the software can be observed if the test is failed.
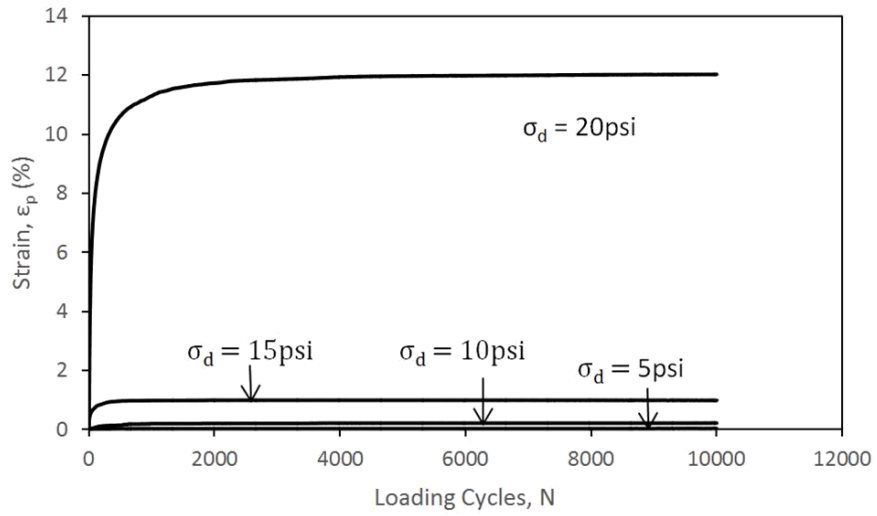
Figure 4.6(a) Strain variations at 5 psi confining pressure
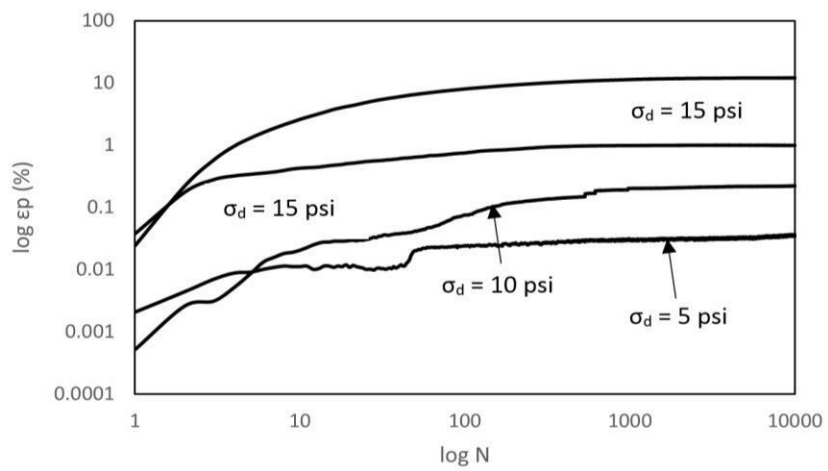
Figure 4.6(b) Strain variations at 5 psi confining pressure
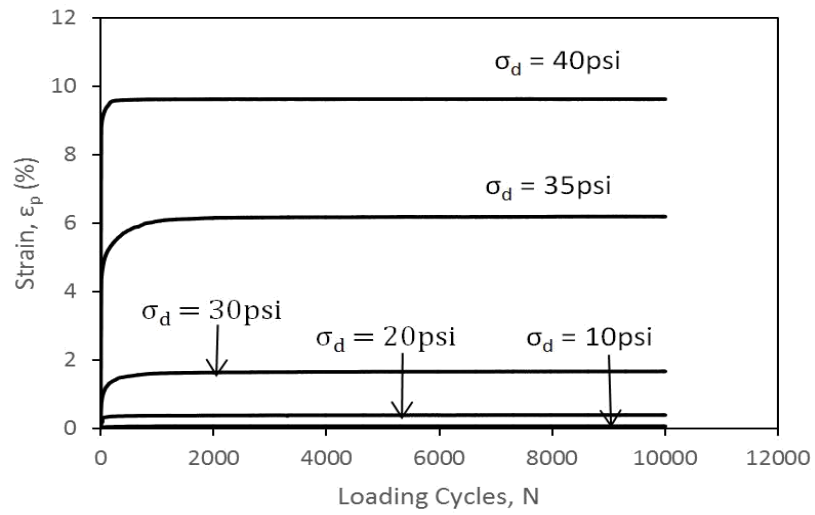
Figure 4.7(a) Strain variations at 10 psi confining pressure
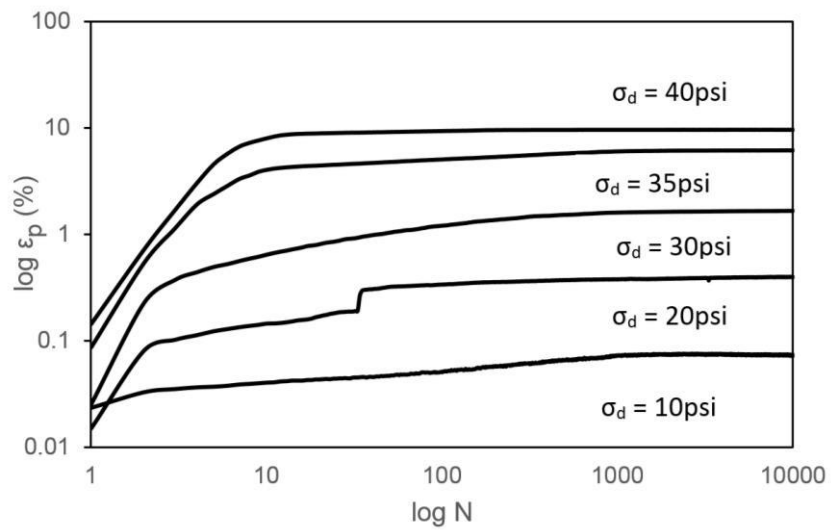
Figure 4.7(b) Strain variations at 10 psi confining pressure
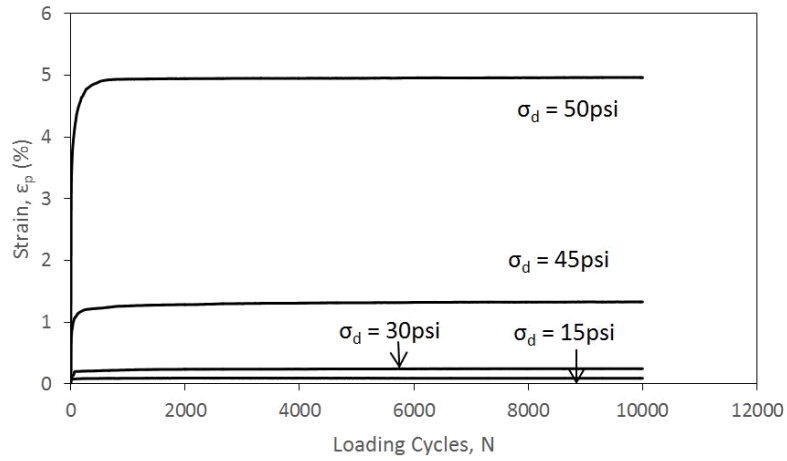
Figure 4.8(a) Strain variations at 15 psi confining pressure
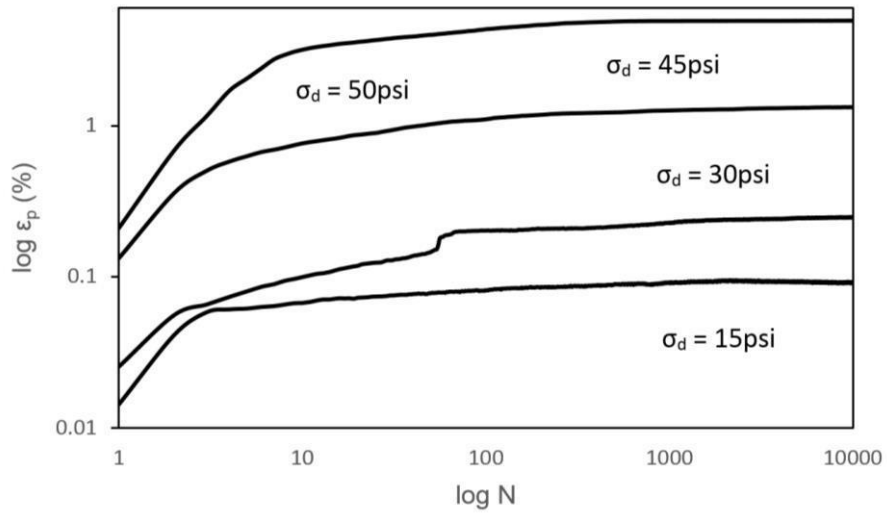
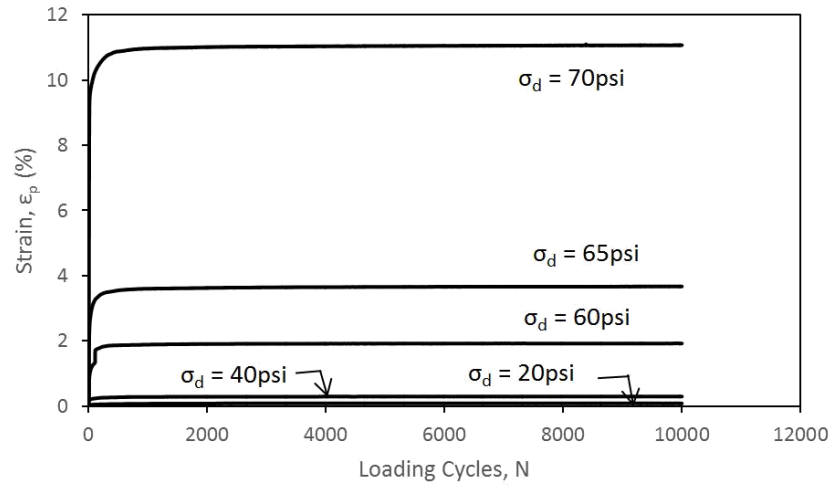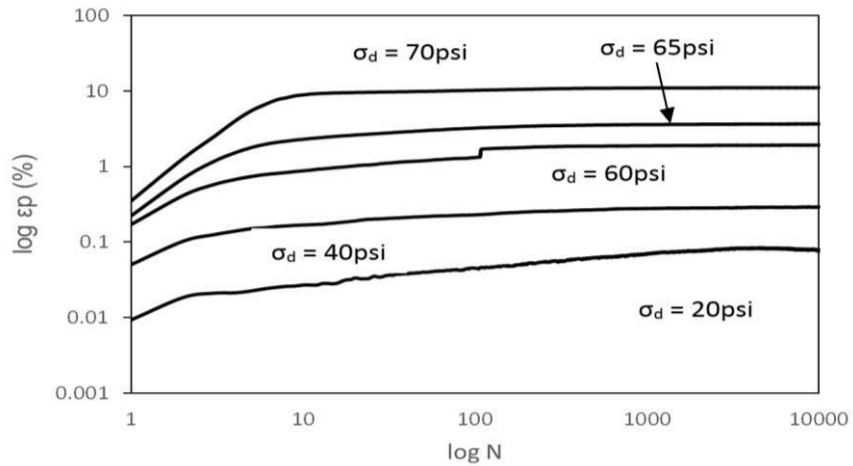**Figure 4.8(b) Strain variations at 15 psi confining pressure**

Figure 4.9(a) Strain variations at 20 psi confining pressure

Figure 4.9(b) Strain variations at 20 psi confining pressure

The relationship of strain with respect to deviator stress was observed. From the Figures 4.6, 4.7, 4.8, and 4.9. It was observed that, as the deviator stress increases, the strain (%) increases at all the confining pressures. A hyperbolic curve was obtained in the graph of the permanent strain. It was also observed that as the confining pressure increases, the permanent strain (%) decreases. Confining pressure is inversely proportional to the permanent strain.

The effect of the number of loading cycles is detailed in log ε_P (%) versus log N graphs from Figures 4.6(b), 4.7(b), 4.8(b), and 4.9(b). The range of loading cycles from 1-100 has more fluctuations when compared to the loading cycles above 100. The strain curve is smooth after 1000 cycles.

Figure 4.10 represents three graphs plotted with respect to the confining pressure. The shear strength of the soil is plotted from the friction angle which is determined from the direct shear test. The maximum stable deviator stress at each confining pressure is the deviator stress before the failure of the sample. The sample fails beyond this cyclic deviator stress. A shear failure envelope develops when the sample fails. The failure envelope is considered to lie between the maximum cyclic deviator stress and the failure deviator stress.
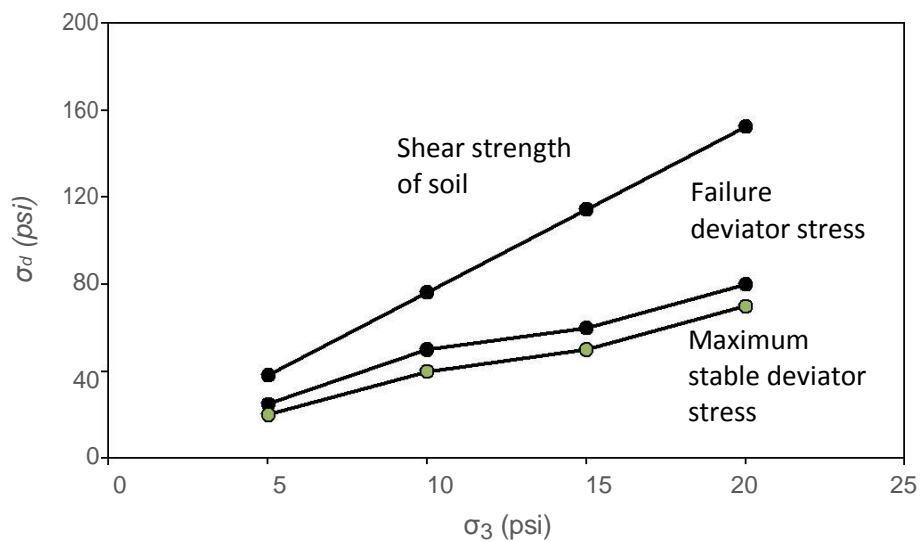
Figure 4.10 Maximum stable, failure deviator stresses and shear strength of soil

4.3.2 Multi-Stage RLT Tests

Multi-stage tests were performed with the same confining pressure and deviator stress as the single-stage tests. The number of loading cycles are 2,500 at each deviator stress. Four tests were conducted with 5 psi, 10 psi, 15 psi and 20 psi. Table 4.1 represents the details of the tests

conducted and the strain results of the multi-stage tests. The strain graphs were plotted for each of the confining pressure and it was observed that the strain increased with the increase of deviator stress as in single-stage tests.
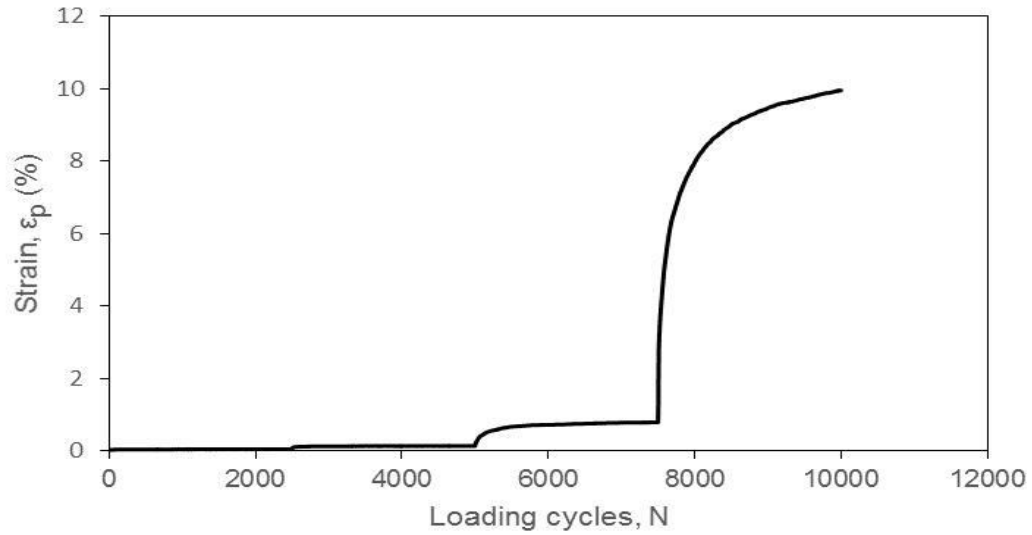
Figure 4.11 Multi-stage test with 5 psi confining pressure
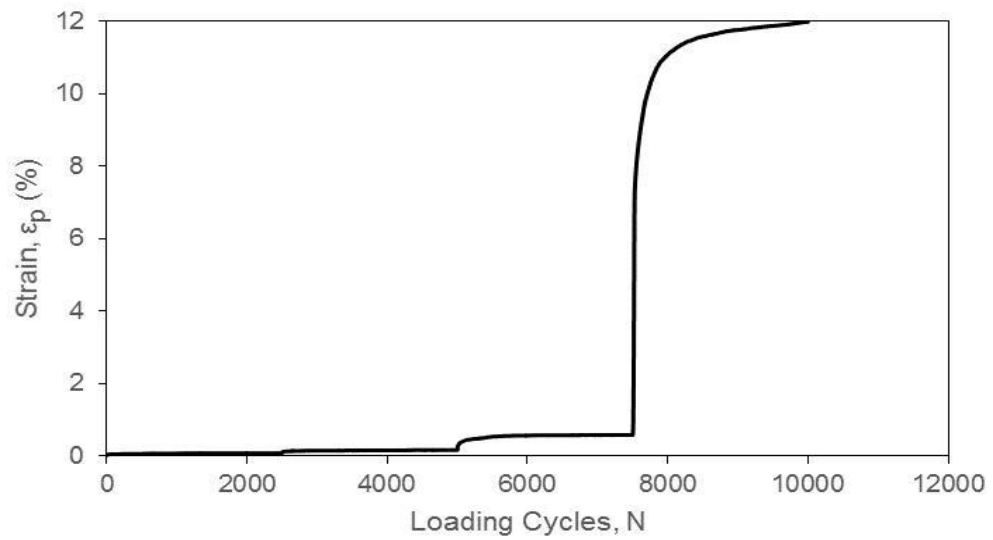
Figure 4.12 Multi-stage test with 10 psi confining pressure
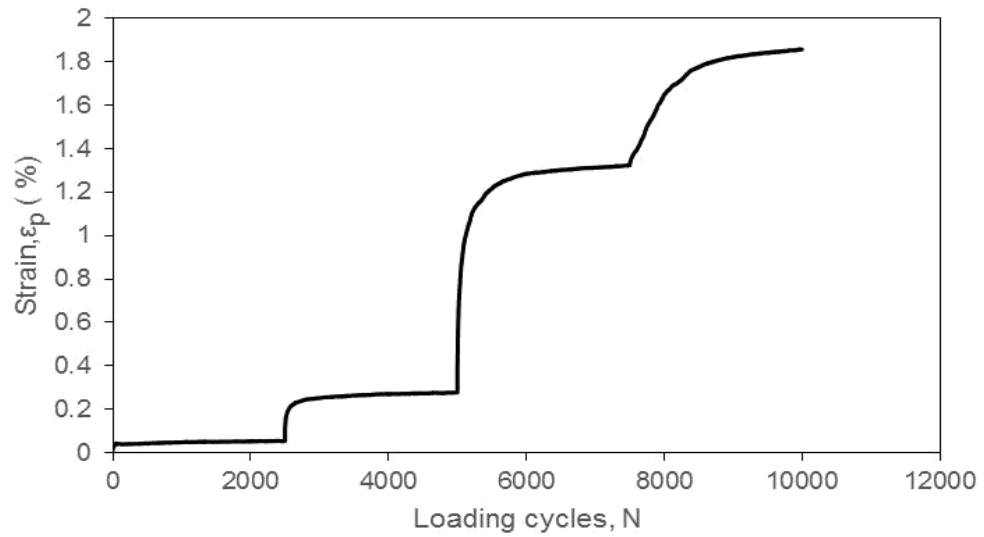
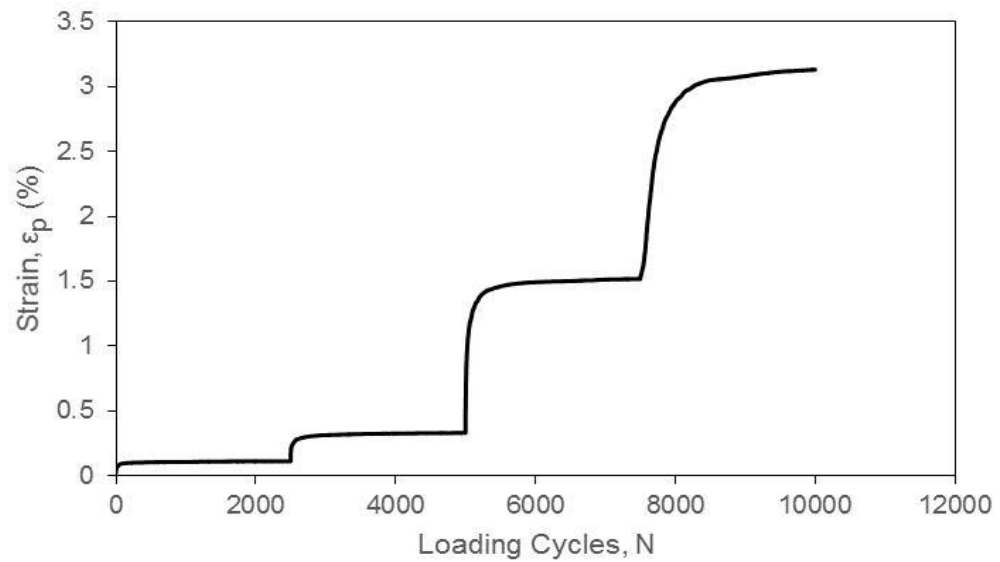**Figure 4.13 Multi-stage test with 15 psi confining pressure**

Figure 4.14 Multi-stage test with 20 psi confining pressure

The increase in strain at each deviator stress was observed from the Figures 4.10, 4.11, 4.12, and 4.13. The strain results from the single-stage tests at 2500 loading cycles were compared to the strain results in multi stage tests. This comparison was detailed in Table 4.1. The strain was similar at low deviator stresses as the effect of the number of loading cycles is low. As the deviator stress increases, there is a difference in the strain. This is due to the loading cycles applied. As there are 7,500 more loading cycles in single-stage test, the strain increases.

Table 4.1 Multi-Stage Test Data

σ_3 (psi)	σ_d (psi)	Strain in single stage tests@ 2500 (%)	Strain in multi stage tests (%)
	5	0.031	0.038
5	10	0.211	0.129
	15	0.995	0.785
	20	11.824	9.961
	10	0.075	0.070
10	20	0.392	0.154
	30	1.649	0.572
	40	9.619	11.992
	15	0.093	0.054
15	30	0.238	0.276
	45	1.294	1.325
	50	4.947	1.857
	20	0.080	0.110
20	40	0.283	0.329
	60	1.914	1.517
	70	11.025	3.132

4.4 Development of Permanent Deformation Model

The data obtained from the tests was analyzed using a regression model developed in this research. The literature review revealed several models developed by some researchers. However,

none of the existing models is able the fit the test curves obtained in this study. Based on the shape of the permanent deformation test curves, a hyperbolic equation was proposed in this study.

Equation 4.1 represents a model which relates the permanent strain and the number of loading cycles. It contains three parameters a, b, and c, which are related to confining pressure and deviator stress.

$$= - \qquad \underline{\qquad} \qquad \text{Equation 4.1}$$

The physical meanings of the parameters a, b, c are discussed below. The parameter "a" represents the ultimate permanent strain at infinite number of load cycle. The parameter "b" is the increment factor which displaces the graph. With the variation of "b", the best fit curve fluctuates from the original test curve. The parameter "c" represents the difference between the ultimate permanent strain and the initial permanent strain. It was observed that "c" does not affect the model as significantly as the other parameters. Best fit curves were plotted for all the strain graphs obtained from which the parameters a, b and c were obtained for each test. The details were presented in Table 4.2.

Table 4.2 Best Fit Parameters

σ_3 (psi)	σ_d (psi)	σ_d/σ_3	Single-stage			Multi-stage			Converted Single-stage		
			a	b	c	a	b	c	a	b	c
5	5	1.0	0.04	0.24	0.038	0.04	0.2	0.04	0.0004	0.007	0.195
5	10	2.0	0.14	0.26	0.116	0.13	0.15	0.12	0.001	0.024	0.146
5	15	3.0	0.8	0.27	0.58	0.6	0.08	0.58	0.006	0.109	0.078
5	20	4.0	10	0.37	9.4	10.5	0.085	10.45	0.102	1.909	0.083
10	10	1.0	0.08	0.23	0.06	0.11	0.11	0.098	0.0006	0.020	0.107
10	20	2.0	0.42	0.25	0.405	0.2	0.045	0.183	0.004	0.036	0.044
10	30	3.0	1.75	0.23	1.72	0.91	0.07	0.9	0.019	0.165	0.068
10	35	3.5	5.8	0.4	5.6	-	-	-	-	-	-
10	40	4.0	10	0.48	9.8	10	0.19	9.98	0.106	1.818	0.185
15	15	1.0	0.098	0.31	0.08	0.09	0.11	0.08	0.0009	0.016	0.107
15	30	2.0	0.25	0.2	0.22	0.4	0.09	0.35	0.002	0.073	0.088
15	45	3.0	1.35	0.41	1.25	1.39	0.099	1.355	0.014	0.253	0.097
15	50	3.3	4.9	0.3	4.7	1.99	0.03	1.98	0.051	0.362	0.029
20	20	1.0	0.09	0.15	0.08	0.14	0.2	0.12	0.0009	0.025	0.195
20	40	2.0	0.3	0.34	0.25	0.36	0.1	0.31	0.0027	0.065	0.098
20	60	3.0	2	0.3	1.83	1.65	0.15	1.6	0.0198	0.300	0.146
20	65	3.3	3.8	0.43	3.58	-	-	-	-	-	-
20	70	3.5	11.5	0.35	11.4	3	0.08	2.99	0.1231	0.545	0.078

Best fit models were presented in Figures 4.13, 4.14, 4.15 and 4.16 for confining pressures of 5 psi, 10 psi, 15 psi and 20 psi respectively.
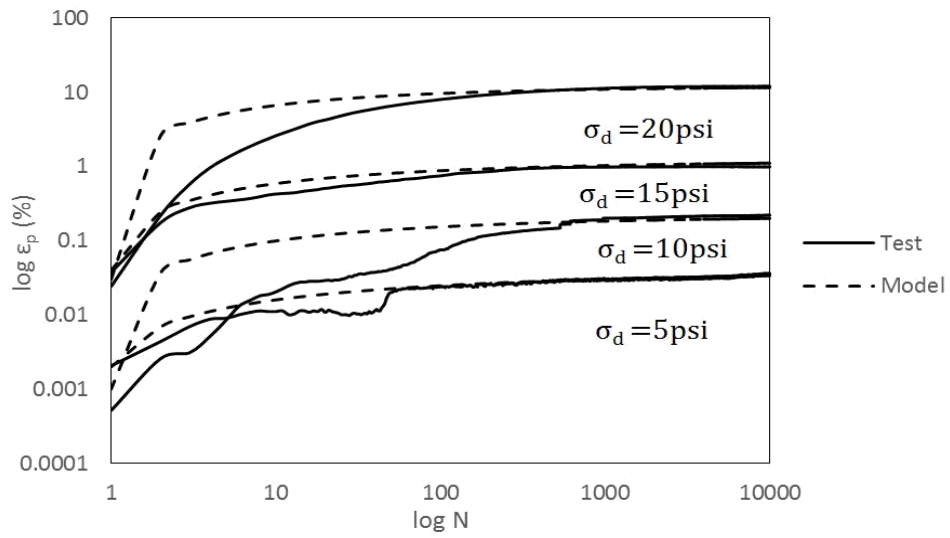
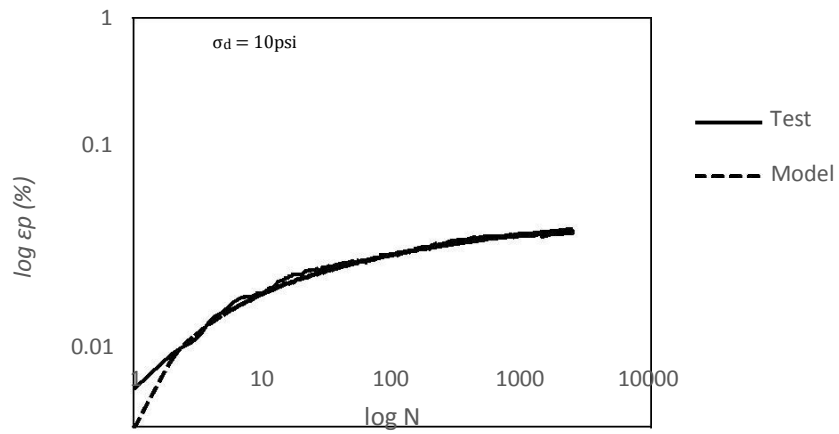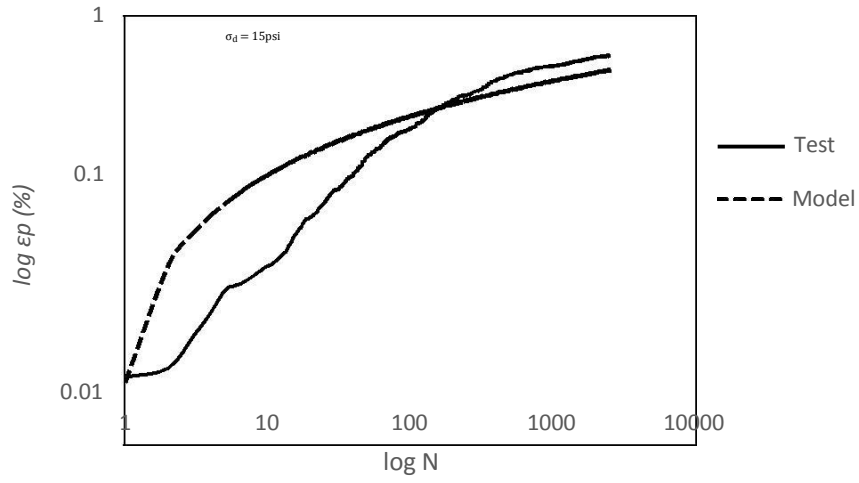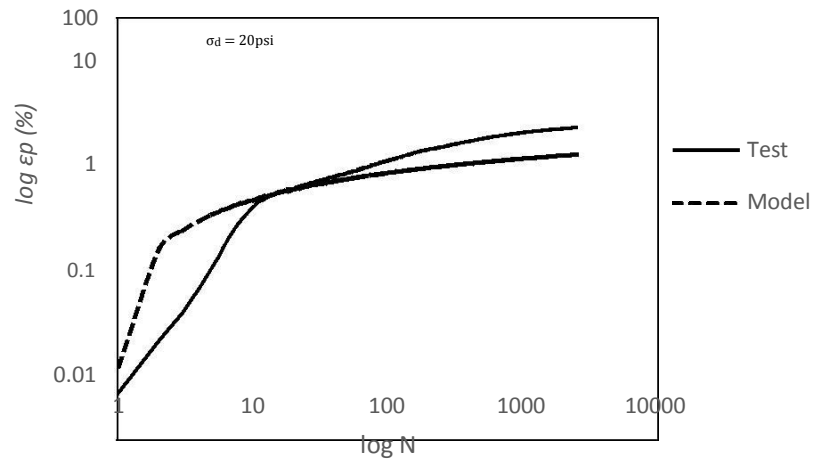**Figure 4.15 Test and best fit curves with a confining pressure of 5 psi**
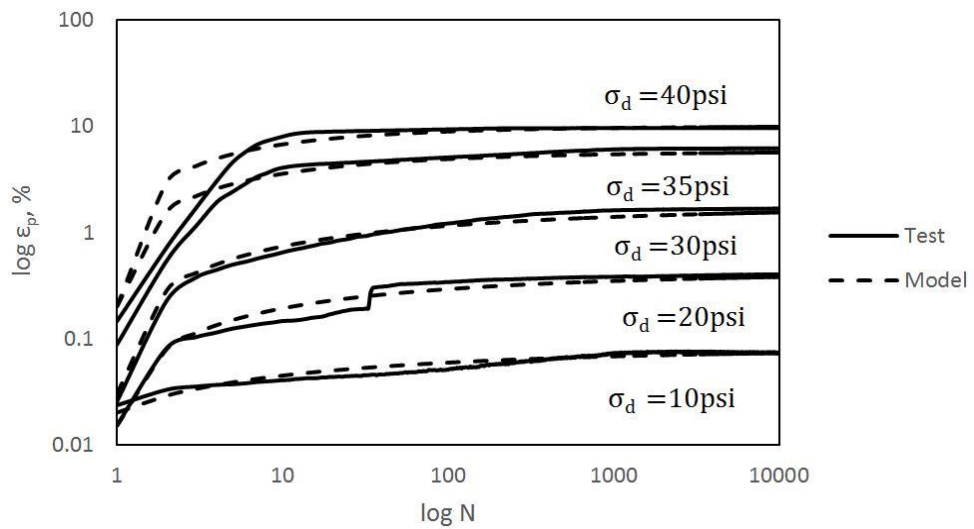
Figure 4.16 Test and best fit curves with a confining pressure of 10 psi
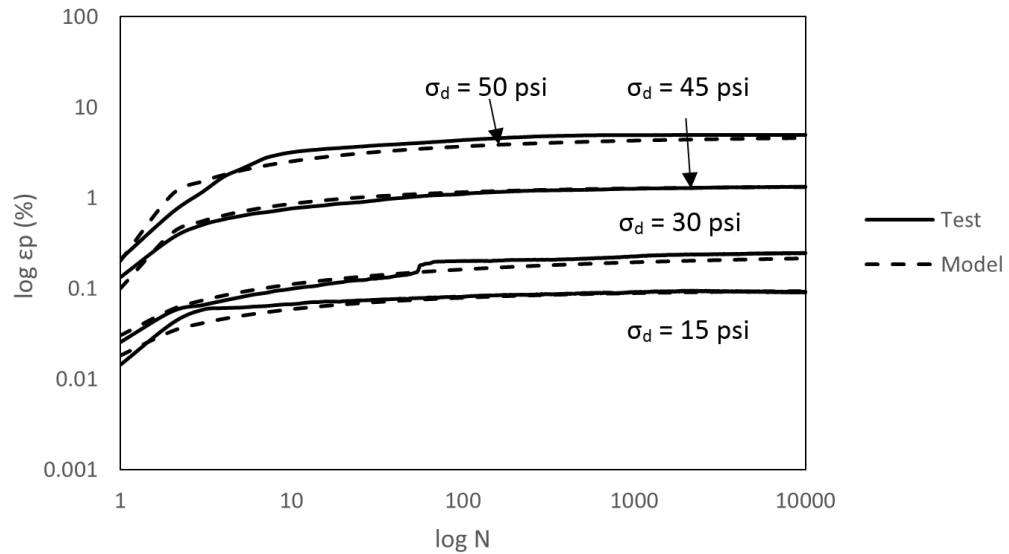
Figure 4.17 Test and best fit curves with a confining pressure of 15 psi
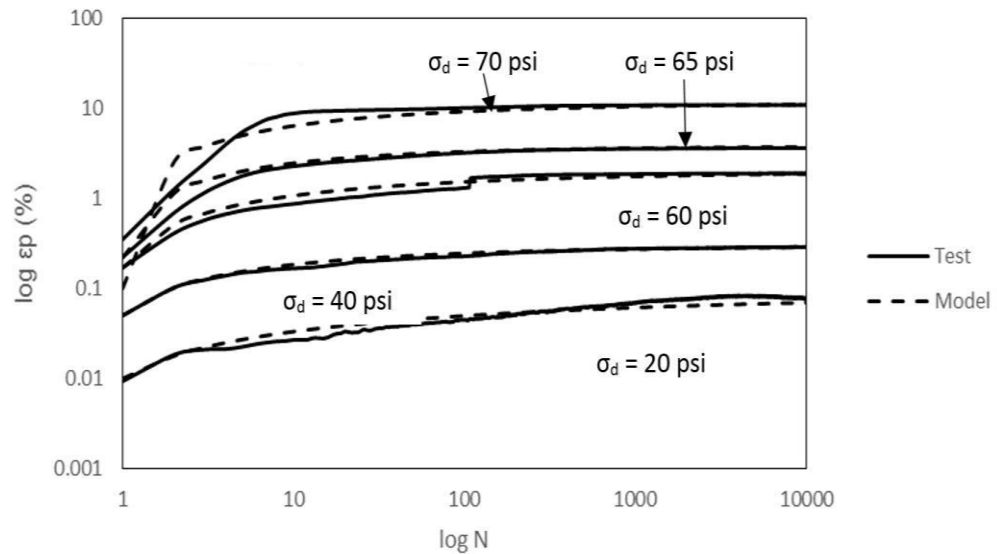
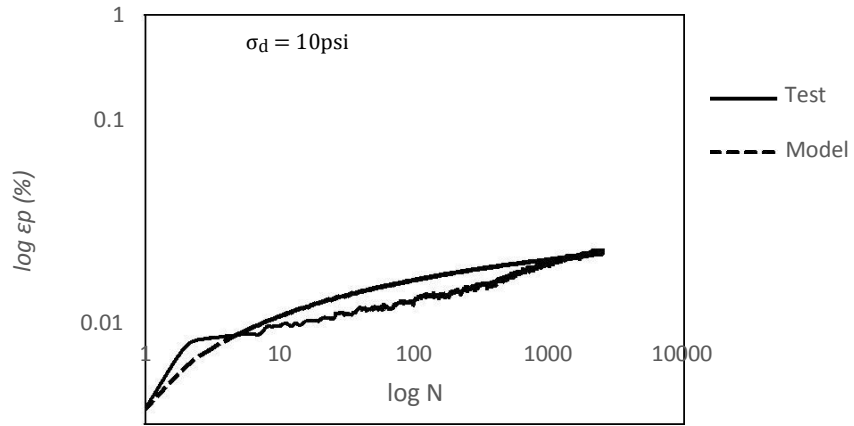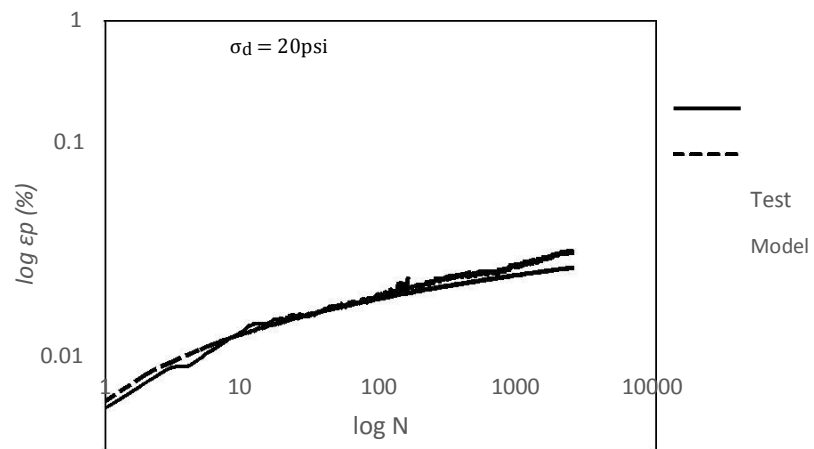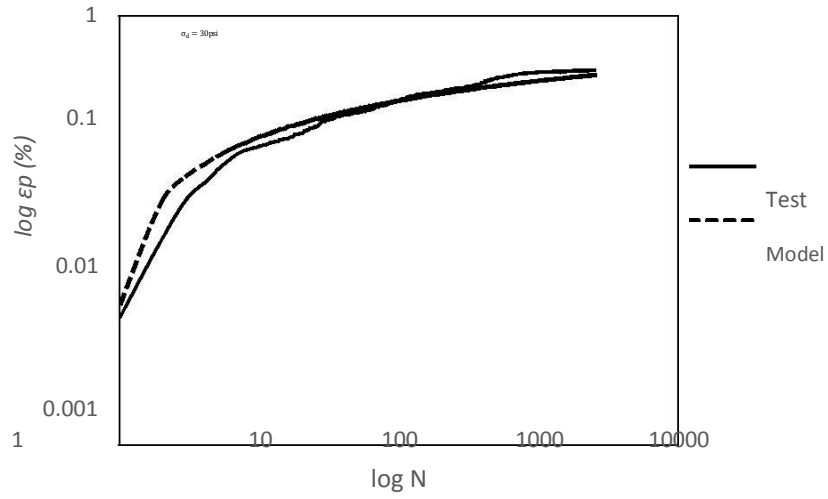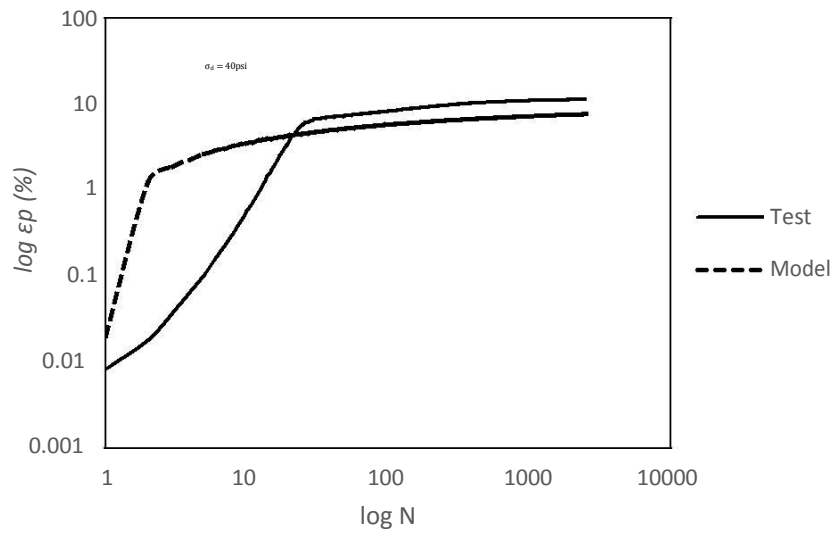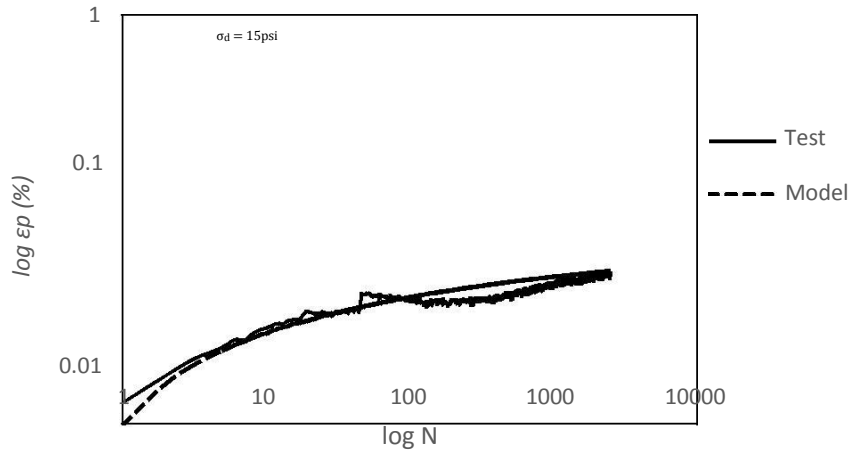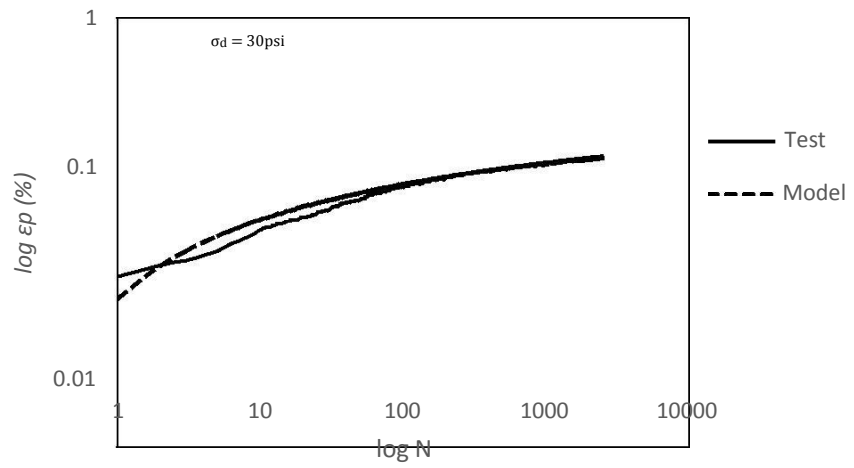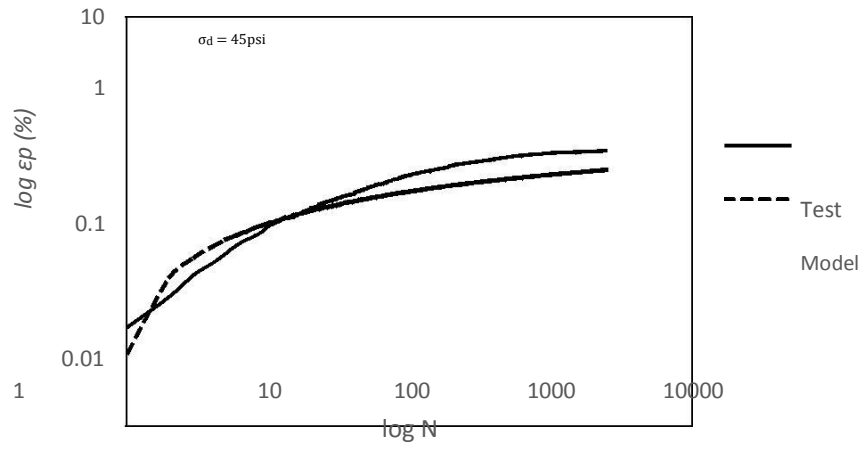**Figure 4.18 Test and best fit curves with a confining pressure of 20 psi**

Best fit curves were plotted for the multi-stage tests at each deviator stresses. Figures 4.19, 4.20, 4.21 and 4.22 represents the best fit models. It was observed that at the highest deviator stress at

each confining pressure the curve does not follow a hyperbolic pattern. Hence, the best fit curve was not accurate.
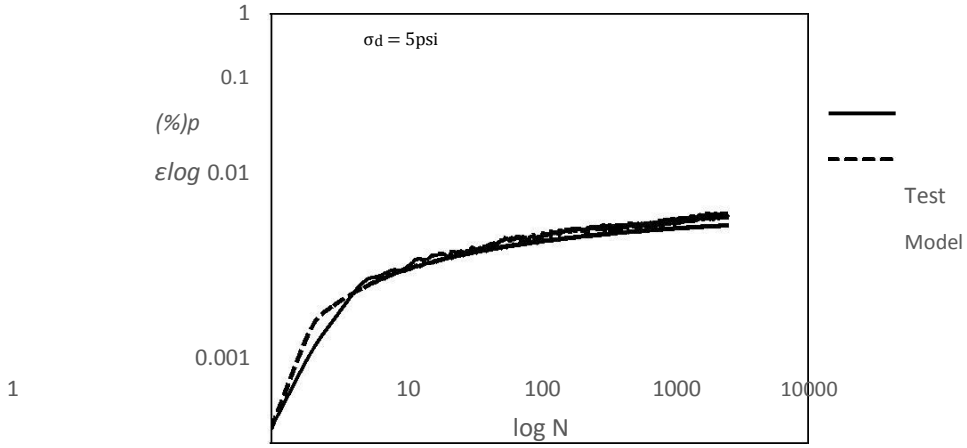
Figure 4.19 (a) Multi-stage best fit curves with a confining pressure of 5 psi

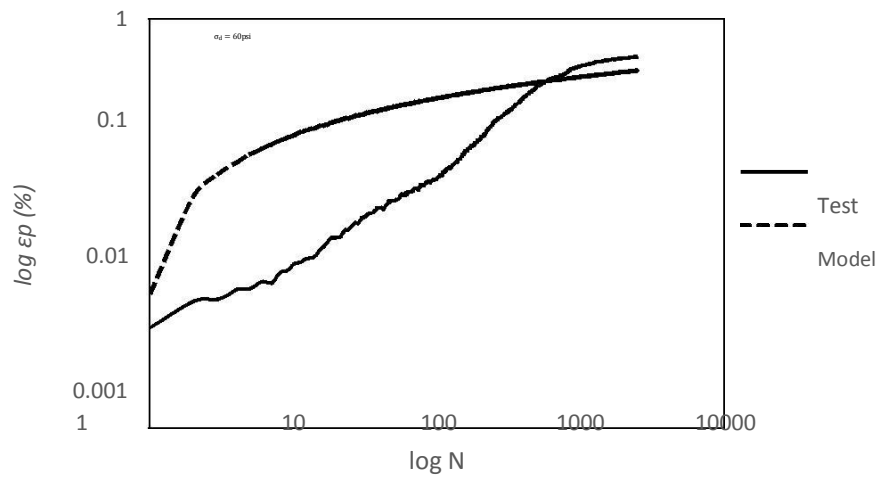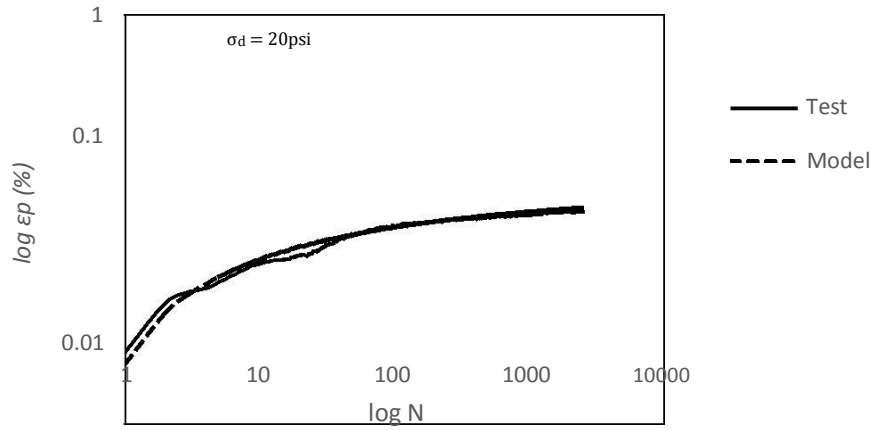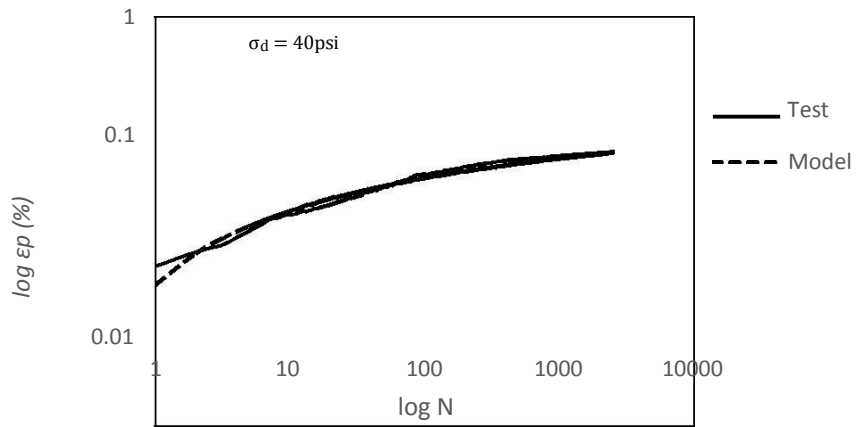**Figure 4.19 (b) Multi-stage best fit curves with a confining pressure of 5 psi**

σ_d = 15psi

Test
Model

log εp (%)

log N

Figure 4.19 (c) Multi-stage best fit curves with a confining pressure of 5 psi

σ_d = 20psi

Test
Model

log εp (%)

log N

Figure 4.19 (d) Multi-stage best fit curves with a confining pressure of 5 psi

Figure 4.20 (a) Multi-stage best fit curves with a confining pressure of 10 psi

Figure 4.20 (b) Multi-stage best fit curves with a confining pressure of 10 psi

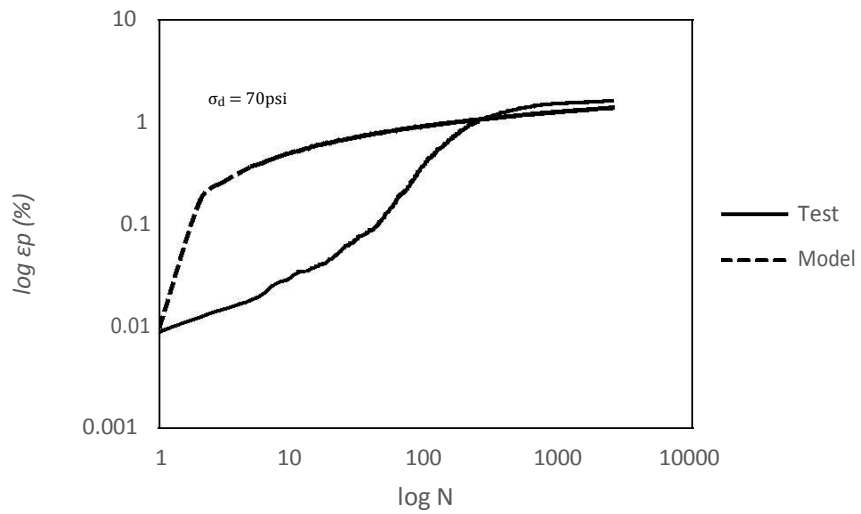**Figure 4.20 (c) Multi-stage best fit curves with a confining pressure of 10 psi**

Figure 4.20 (d) Multi-stage best fit curves with a confining pressure of 10 psi

Figure 4.21 (a) Multi-stage best fit curves with a confining pressure of 15 psi

Figure 4.21 (b) Multi-stage best fit curves with a confining pressure of 15 psi

Figure 4.21 (c) Multi-stage best fit curves with a confining pressure of 15 psi

Figure 4.21 (d) Multi-stage best fit curves with a confining pressure of 15 psi

Figure 4.22 (a) Multi-stage best fit curves with a confining pressure of 20 psi

Figure 4.22 (b) Multi-stage best fit curves with a confining pressure of 20 psi
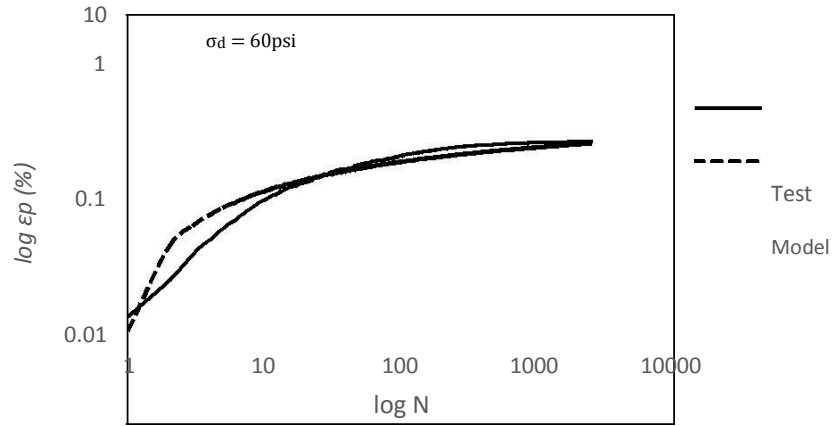
Figure 4.22 (c) Multi-stage best fit curves with a confining pressure of 20 psi

Figure 4.22 (d) Multi-stage best fit curves with a confining pressure of 20 psi

The relationship between "a" and the confining pressure and deviator stress was analyzed. Figure 4.23 represents the relationship between log a and the deviator stress. Figure 4.24 represents the represents the relationship between log b and the deviator stress. The graphs follow a similar exponential pattern.

The relationship between "log a" and the ratio of deviator stress to confining pressure shows a linear relationship. An exponential equation was obtained from the data. Similarly, the log b versus (σ_d/σ_3) plot shows a linear relationship and an exponential equation was obtained which was used to develop an equation for "b".
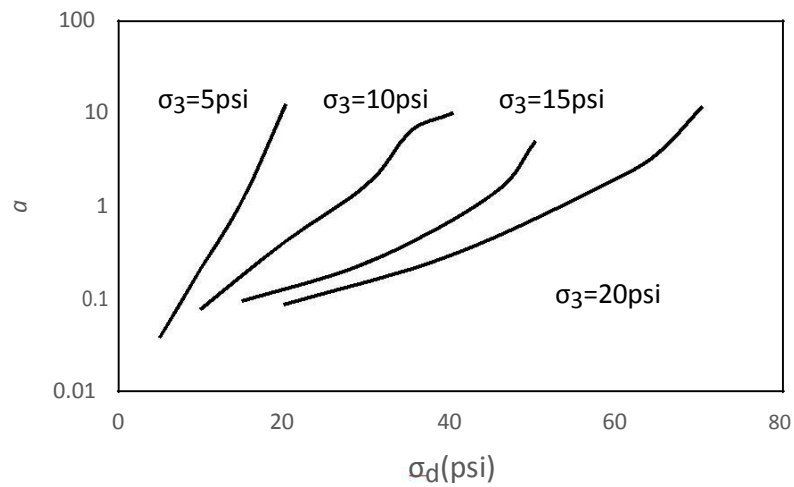
Figure 4.23 Correlation between "log a" and "σ_d"
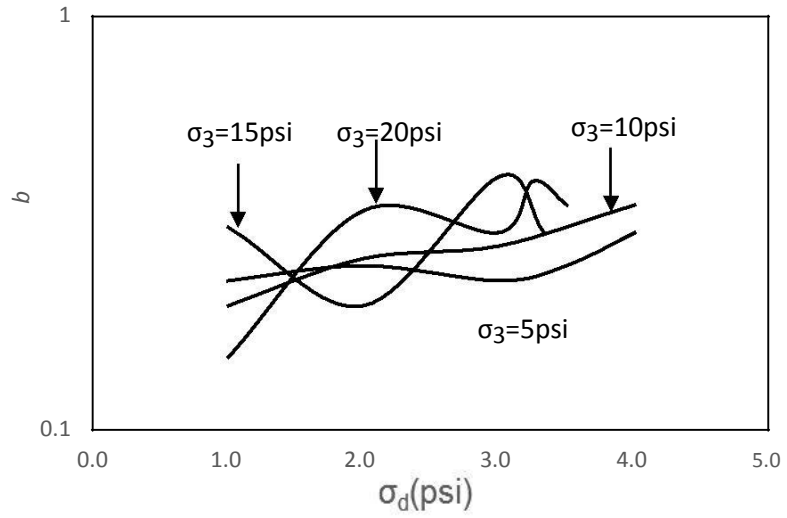
Figure 4.24 Correlation between "log b" and "σ_d"

$$a = 0.0108e^{1.7144(\sigma_d/\sigma_3)}$$

$$b = 0.1818e^{0.1812(\sigma/\sigma_3)}$$
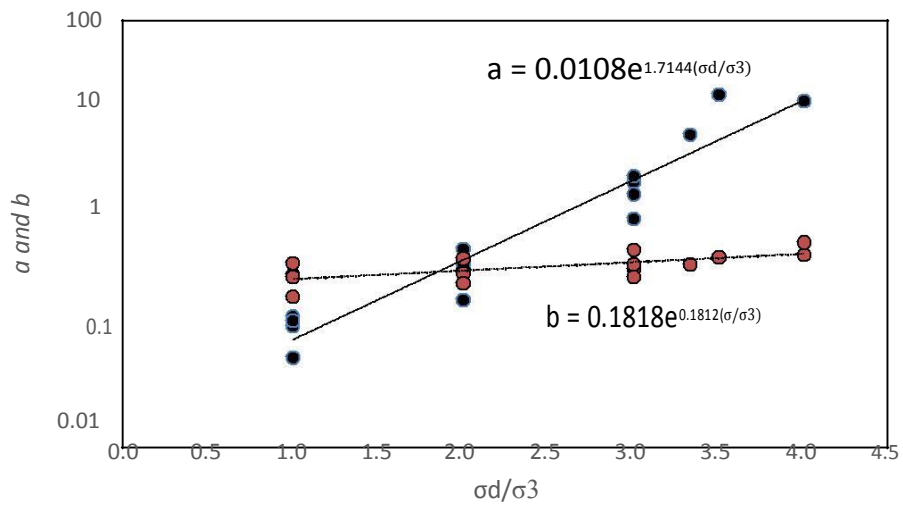
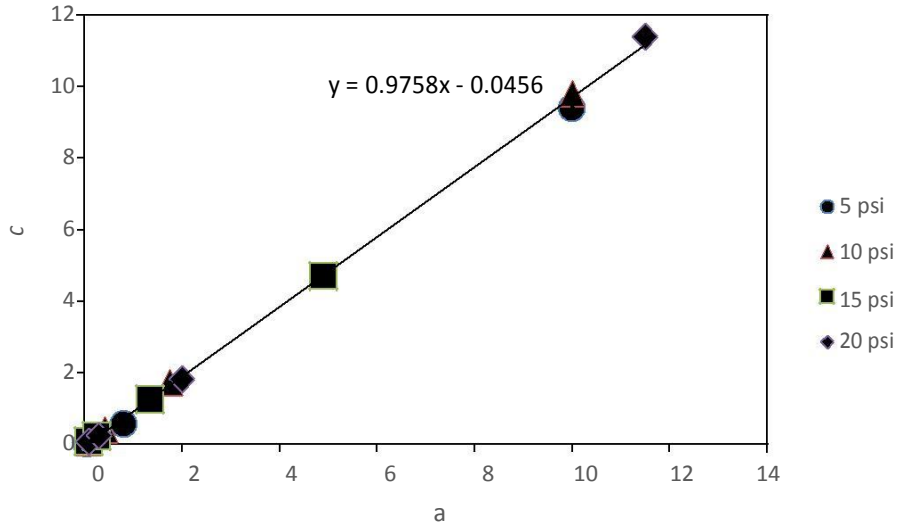**Figure 4.25 log a and log b versus (σ_d/σ_3)**

Figure 4.26 c versus a

Figure 4.25 represents the relation of log a and log b with the ratio of deviator stress to confining pressure. The parameters "a" and "c" are interrelated since they are derived from the permanent strain which is detailed in Figure 4.26.

$$a = 0.0108^{.7144} \qquad \qquad \qquad \text{Equation 4.2}$$

$$b = 0.1818 \qquad \qquad \qquad \text{Equation 4.3}$$

$$c = 0.9758*a \qquad \qquad \text{Equation 4.4}$$

Equations 4.2, 4.3 and 4.4 represent the relation of the parameters with the confining pressure and deviator stress. The factors obtained from the equations are presented below.

$k_1 = 0.0108$, $k_2 = 1.7144$, $k_3 = 0.1818$, $k_4 = 0.1812$, $k_5 = 0.9758$

$$a = 1 \quad ^2 \, (\,)$$

$$b = 3 \qquad (\text{—})$$

c = 5 * a

These parameters can be used as the standard factors for a granular material with the confining pressures and the deviator stresses used in this study.

4.5 Permanent Deformation Test Results-Multi-Stage

Multi-stage tests were conducted at four deviator stresses for each confining pressure as mentioned in Table 4.1. The purpose of conducting these tests with the stresses similar to that of single-stage tests is to compare and study the results.
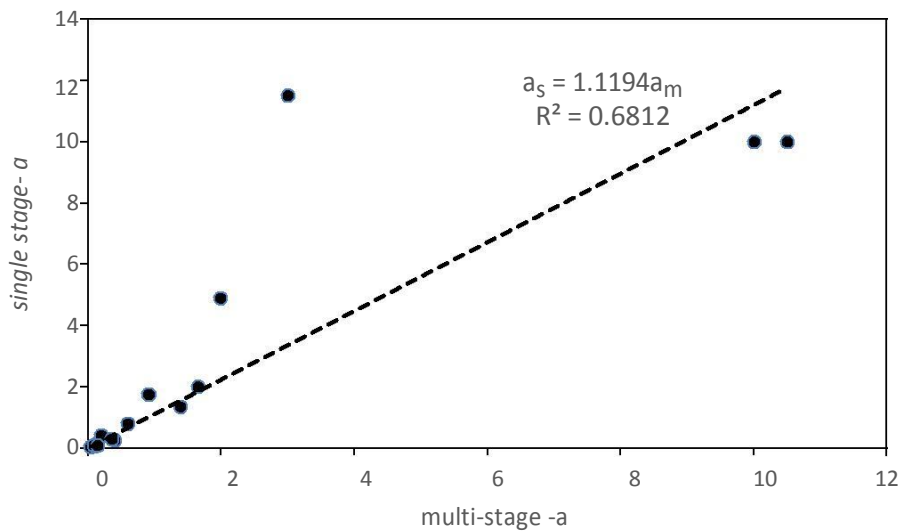

Figure 4.27 Comparison of "a" values of single stage and multi stage tests
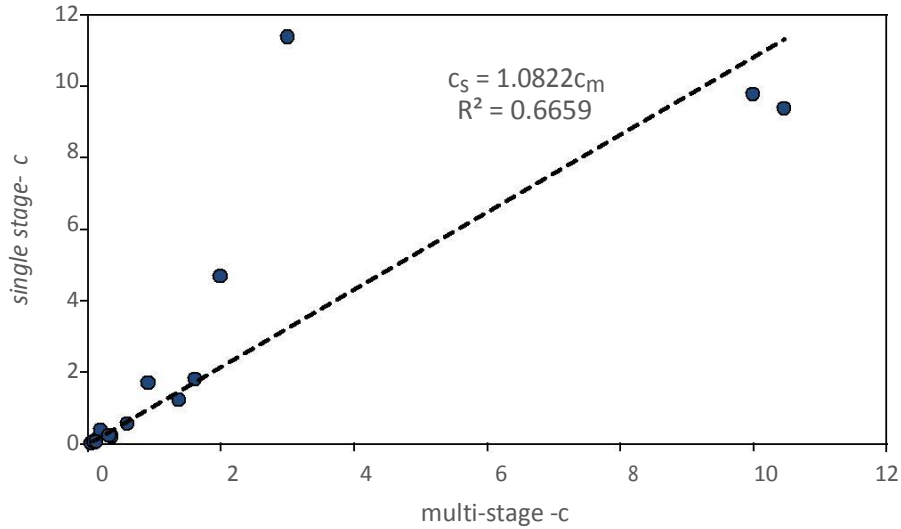
Figure 4.28 Comparison of "c" values of single stage and multi stage tests

From the Figures 4.27 and 4.28, the factors to convert the multi stage parameters to single stage parameters were obtained. Table 4.3 shows the details of the converted parameters by using the following factors. For the parameter "a", the factor is 1.1194. For the parameter "c", the factor is 1.0822.

Figures 4.29, 4.30, 4.31, and 4.32 represent the best fit curves of the single-stage tests. The converted parameters were calculated from the multiplication factors obtained from the multi-stage tests.
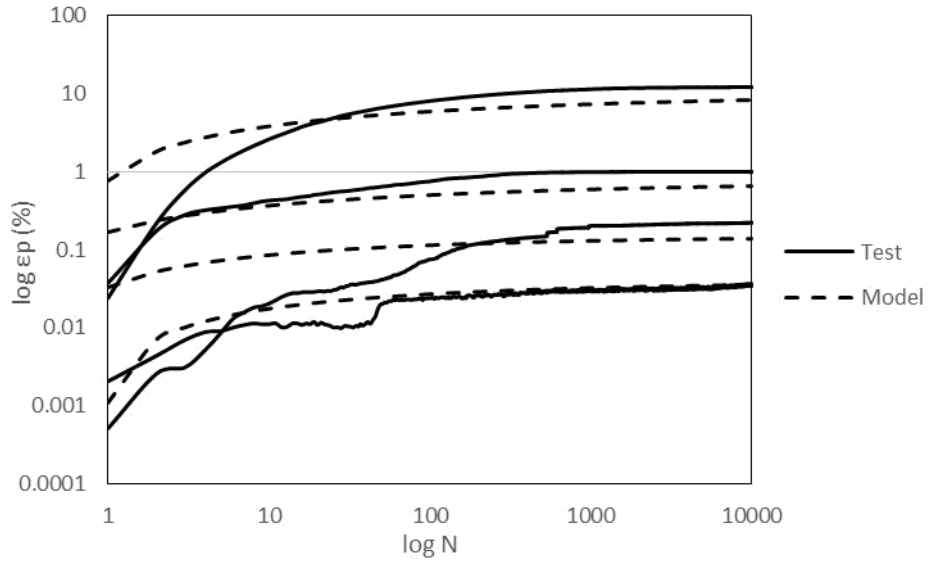
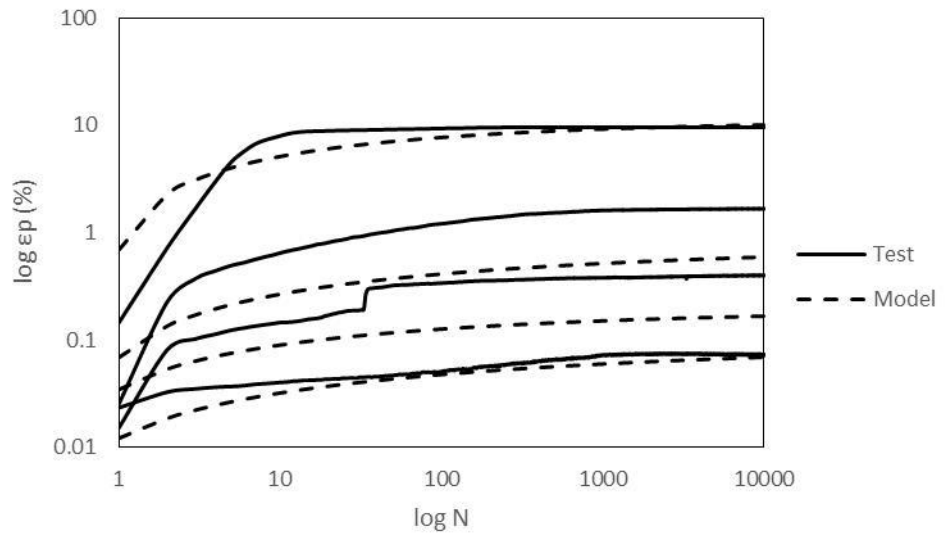**Figure 4.29 Best fit curves for converted single stage tests with 5psi confining pressure**

Figure 4.30 Best fit curves for converted single stage tests with 10psi confining pressure
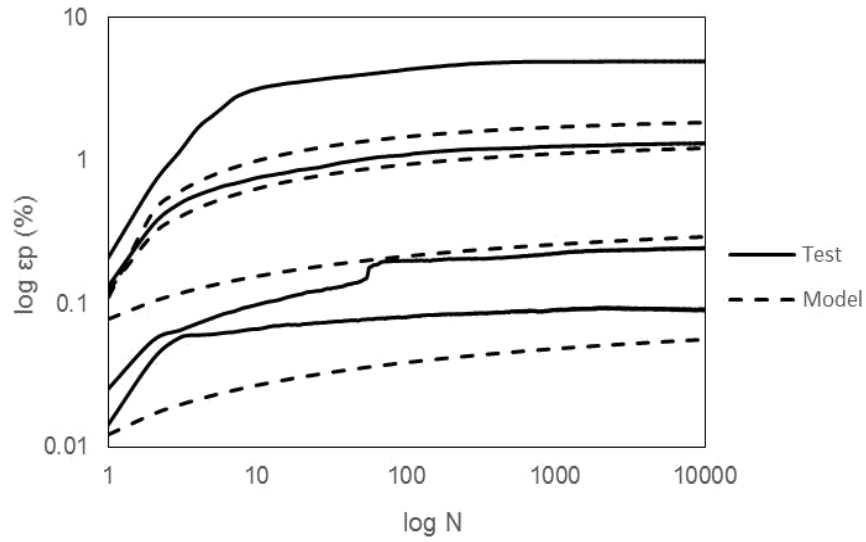
Figure 4.31 Best fit curves for converted single stage tests with 15psi confining pressure
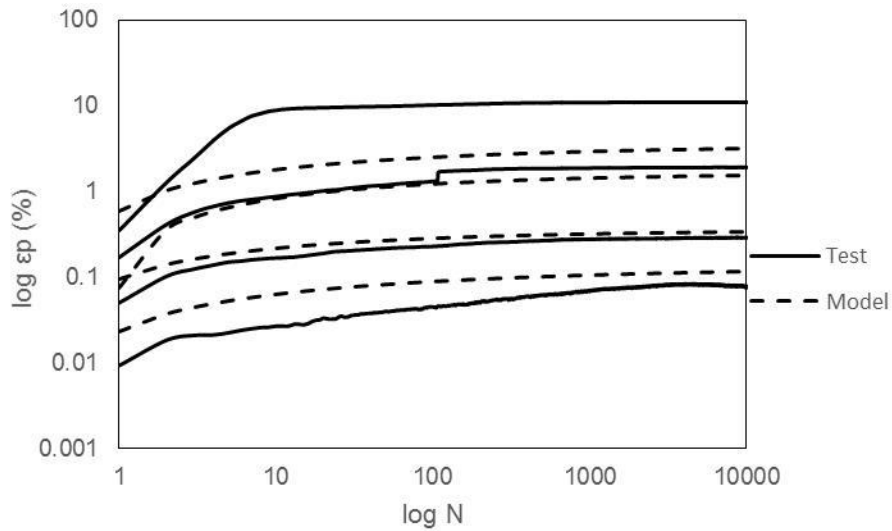

Figure 4.32 Best fit curves for converted single stage tests with 20psi confining pressure

4.6 Suggested Permanent Deformation Procedure

Since no standard is recommended for permanent deformation, a procedure was suggested under some limitations. Table 4.3 suggests the loading table with varying deviator stresses and loading cycles at each confining pressure. The confining pressures were suggested similar to those

58

pressures used in this study. Multi-stage tests were recommended since single-stage tests are time-consuming. A procedure was recommended to determine the permanent deformation which is detailed below.

1. Perform the multi-stage tests with the confining pressures mentioned in the suggested loading table 4.3. Plot a graph of the permanent strain (%) with the number of loading cycles (N). The multi-stage tests were recommended since the single-stage tests were time-consuming.

2. The parameters a, b, and c are to be obtained by curve fitting. Equation 4.1 is the model developed for curve fitting. These parameters obtained from the multi-stage analysis should be converted to the single-stage using the factors obtained from the Figures 4.23, 4.24, and 4.25.

3. Graphs should be plotted between the parameters a, b, and c as plotted in Figures 4.21 and 4.22. k_1, k_2, k_3, k_4, and k_5 were to be obtained from the equations 4.2, 4.3 and 4.4.

From the comparison of the single stage tests and multi stage tests, it was observed that the initial strain was not as affected as the final stages. Hence, the increment in deviator stress is low to determine the failure of the sample. The ratio of the static load before failure point and the shear strength was calculated and it ranges from 0.52-0.65. The ratio between the maximum stable deviator stress and the shear strength was observed to be 0.46-0.52. The static load strength was compared to the cyclic deviator stress, which ranges from 45%-65%.

\

Table 4.3 Suggested Loading Table

	Confining Pressure, σ_3 (psi)				Loading Cycles, N
	5	10	15	20	
————	0.15	0.15	0.15	0.15	2,500
	0.3	0.3	0.3	0.3	2,500
	0.45	0.45	0.45	0.45	2,500
	0.5	0.5	0.5	0.5	2,500
	0.6	0.6	0.6	0.6	2,500

The suggested loading table recommends increase in the ratio of the deviator stress in this study to the deviator stress before failure, as the deviator stress increases. The limitation for this suggested loading table is that it may not be used for other soils. Since, this study deals with unbound granular material, any other soil needs to be tested with the above loading table.

CHAPTER V

CONCLUSIONS AND RECOMMENDATIONS

5.1 Conclusions

Permanent deformation tests were conducted on a poorly graded silica sand in the laboratory to characterize the behavior of unbound granular materials. Both single-stage and multi-stage tests were conducted at different load conditions. The physical properties of the soil were also tested. Based on the test data and analyses, the following conclusions can be drawn:

1. Repeatability tests were conducted with and without preconditioning stages. The permanent deformation test results were considered to be repeatable. The preconditioning stage seemed to have an impact on the repeatability of the permanent deformation test.

2. From the single-stage permanent test results, the permanent strain of the granular soil increases with the number of load cycles. The relationship between the permanent strain and the number of load cycle followed a hyperbolic curve. The proposed regression model can simulate the permanent test results very well.

3. The permanent deformation behavior of the granular soil is stress-dependent. The permanent strain of the granular soil increases with the deviator stress and decreases with the confining stress.

4. There exists a maximum cyclic deviator stress level at each confining pressure beyond which the soil will develop shear failure under the cyclic load. For the poorly graded sand

61

5. tested in this study, the maximum cyclic deviator stress was about 45% to 65% of the static load strength of the soil at different confining stress levels.

6. The multi-stage permanent deformation test results seemed to correlate well with individual single-stage permanent deformation tests at the same stress level. Multi-stage permanent deformation test can be used to estimate the parameters for the proposed permanent deformation model.

5.2 Recommendations

This permanent deformation model and the recommended multi-stage permanent deformation test procedure were developed based on one soil type (a poorly graded sand). Further verification tests are needed using different granular materials such as aggregate and well graded sand. The relationship used in the proposed permanent deformation model also need to be further improved by more test data on a variety of granular materials.

REFERENCES

1. Allen, J. J., and Thompson, M. R. (1974). ''Resilient response of granular materials subjected to time dependent lateral stresses.'' *Transp. Res. Rec. 510, Transportation Research Board, Washington, D.C., 1–13.*

2. Austin, A. (2009). "Fundamental characterization of unbound base course materials under cyclic loading." M.S thesis, Louisiana State University., Louisiana.

3. Barksdale, R. D. (1972). ''Laboratory evaluation of rutting in basecourse materials.'' *Proc., 3rd Int. Conf. on Struct. Des. of Asphalt Pavements*, 161–174.

4. Brown and Foo (1989). "Evaluation of Variability in Resilient Modulus Test Results". *National Center for asphalt Technology,* NCAT Report No.91-6.

5. Brown, S. F., and Hyde, A. F. L. (1975). ''Significance of cyclic confining stress in repeated-load triaxial testing of granular material.'' *Transp. Res. Rec. 537, Transportation Research Board, Washington, D.C.,* 49– 58.

6. Cerni, G., et al. (2011). "Characterization of permanent deformation behavior of unbound granular materials under repeated triaxial loading.*" Construction and Building Materials,* 28 (2012), 79-87.

7. Chen, Q., et al. (2013). "Shakedown Analysis of Geogrid-Reinforced Granular Base Material.*" J. Mater. Civ. Eng.,* 2013, 25: 337-346.

8. Elliot, R. P., et al. (1998). "Permanent Deformation of Subgrade Soils". *Mack-Blackwell Rural transportation Study Center and Arkansas Highway and Transportation Department.*

9. *Flexible Pavements, Proc., Eur. Symp. Euroflex 1993, A. G. Correia, ed., Balkema, Rotterdam, The Nether-lands,* 53–64.

10. Guimaraes, A. C. R. and Motta L. M. G. (2008). "A study on permanent deformation of lateritic soils including the shakedown concept." *Advances in Transportation Geotechnics, Taylor and Francis Group, London,* 149-155.

11. Hicks, R. G. (1970). ''Factors influencing the resilient properties of granular materials,'' PhD thesis, University of California, Berkeley, Berkeley, Calif.

12. Holubec, I. (1969). ''Cyclic creep of granular materials.'' *Rep. No. RR147, Department of Highways, Ontario, Canada.*

13. http://www.pavementinteractive.org/article/subgrade/>13, Accessed November 2014.

14. Jouve, P., Martinez, J., Paute, J. L., and Ragneau, E. (1987). ''Rational model for the flexible pavement deformations.'' *Proc., 6th Int. Conf. on Struct. Des. of Asphalt Pavements, Vol. 1*, 50–64.

15. Khedr, S. (1985). ''Deformation characteristics of granular base course in flexible pavement.'' *Transp. Res. Rec. 1043, Transportation Research Board, Washington, D.C.*, 131–138.

16. Kolisoja, P. (1997). ''Resilient deformation characteristics of granular ma-terials,'' PhD thesis, Tampere University of Technology, Publ. No. 223, Tampere, Finland.

17. Kumar, P., et al. (2006). "Comparative Study of Different Subbase Materials." *J. Mater. Civ. Eng*., 2006, 18:576-580.

18. Lashine, A. K., Brown, S. F., and Pell, P. S. (1971). ''Dynamic properties of soils.'' *Rep. No. 2, Submitted to Koninklijke/Shell Laboratorium, Dept. of Civ. Engrg., University of Nottingham, Nottingham, England.*

19. Lekarp, F., and Dawson, A. (1998). ''Modelling permanent deformation behaviour of unbound granular materials.'' *Constr. and Build. Mat.,* 12(1), 9–18.

20. Lekarp, F., et al. (2000). "State of the Art. I: Resilient Response of Unbound Aggregates." *J. Transp. Eng*., 2000, 126:66-75.

21. Lekarp, F., et al. (2000). "State of the Art. II: Permanent strain Response of Unbound Aggregates." *J. Transp. Eng*., 2000, 126:76-83.

22. Lentz, R. W., and Baladi, G. Y. (1981). ''Constitutive equation for per-manent strain of sand subjected to cyclic loading.'' *Transp. Res. Rec. 810, Transportation Research Board, Washington, D.C.,* 50–54.

23. Li, J. (2013). "Permanent deformation and resilient modulus of unbound granular materials." M.S thesis, Iowa State University., Ames, Iowa.

24. Mengelt, M., et al. (2006). *"*Resilient modulus and plastic deformation of soil confined in a geocell.*" Geosynthetics International*, 13, No. 5, 195-205.

25. Monismith, C. L., Seed, H. B., Mitry, F. G., and Chan, C. K. (1967). ''Prediction of pavement deflections from laboratory tests.'' *Proc., 2nd Int. Conf. Struct. Des. of Asphalt Pavements,* 109–140.

26. Morgan, J. R. (1966). ''The response of granular materials to repeated loading.'' *Proc., 3rd Conf., ARRB*, 1178–1192.

27. Pappin, J. W. (1979). ''Characteristics of granular material for pavement analysis,'' PhD thesis, Dept. of Civ. Engrg., University of Nottingham, Nottingham, England.

28. Paute, J. L., Hornych, P., and Benaben, J. P. (1996). ''Repeated load triaxial testing of granular materials in the French network of Labor-atoires des Ponts et Chausse´es.''

Flexible Pavements, Proc., Eur. Symp. Euroflex 1993, A. G. Correia, ed., Balkema, Rotterdam, The Nether-lands, 53–64.

29. Paute, J. L., Hornych, P., and Benaben, J. P. (1996). ''Repeated load triaxial testing of granular materials in the French network of Labor-atoires des Ponts et Chausse´es.'' Rahman, M. A., et al. (2014). "Resilient Modulus and Permanent Deformation Responses of Geogrid-Reinforcement Construction and Demolition Materials." *J. Mater. Civ. Eng*., 2014, 26: 512-519.

30. Seed, H. B., Mitry, F. G., Monismith, C. L., and Chan, C. K. (1965). ''Predictions of pavement deflection from laboratory repeated load tests.*'' Rep. No. TE-65-6, Soil Mech. and Bituminous Mat. Res. Lab., University of California, Berkeley, Berkeley, Calif.*

31. Sweere, G. T. H. (1990). ''Unbound granular basis for roads,'' PhD thesis, University of Delft, Delft, The Netherlands.

32. Thom, N. H., and Brown, S. F. (1988). ''The effect of grading and density on the mechanical properties of a crushed dolomitic limestone.*'' Proc., 14th ARRB Conf., Vol. 14, Part 7,* 94–100.

33. Theyse H. L., Mechanistic-Empirical Modeling of the Permanent Deformation of Unbound Pavement Layers, Proceeding, 8th International Conference on Asphalt Pavements, Seattle, Washington, August 10-14, 1997, pp1579-1594.

34. Uzan, J. (1985). ''Characterization of granular material.*'' Transp. Res. Rec. 1022, Transportation Research Board, Washington, D.C.,* 52–59.

35. Veverka, V. (1979). ''Raming van de spoordiepte bij wegen met een bi-tumineuze verharding.*'' De Wegentechniek,* 24(3), 25–45 (*in Dutch*).

36. Vuong, B. (1992). ''Influence of density and moisture content on dynamic stress-strain behaviour of a low plasticity crushed rock.*'' Rd. and Transp. Res.,* 1(2), 88–100.

37. Wolff and Visser (1994). "Incorporating elasto-plasticity in granular layer pavement design*". Proc. Instn. Civ. Engrs Transp.,* 105 Nov., 259-272.

38. Witczak, M. W., and Uzan, J. (1988). ''The universal airport pavement design system, Report I of IV: Granular material characterization.'' *University of Maryland, College Park, Md.*

39. Wu and Chen (1997). "Prediction of Permanent Deformation of Pavement Base and Subgrade Materials under Accelerated Loading". *ISSN 1997-1400 Int. J. Pavement Res. Technol.* 4(4):231-237.

APPENDICES

A STRAIN, MODULUS AND LOAD GRAPHS

The permanent strain was calculated from the permanent deformation test. Graphs were plotted with permanent strain, strain, modulus and load with the number of loading cycles. The number of loading cycles represents the time. Appendix A shows the graphs for all the tests performed at all the confining pressures of 5psi, 10psi, 15psi and 20psi. Non-linear strain graphs were obtained in all the tests. The range of the load (lb) can be observed from the test graphs.

Confining pressure, (psi)	Deviator Stress, (psi)	Contact pressure (psi)	Number of loading cycles, N
5	5	0.5	10,000

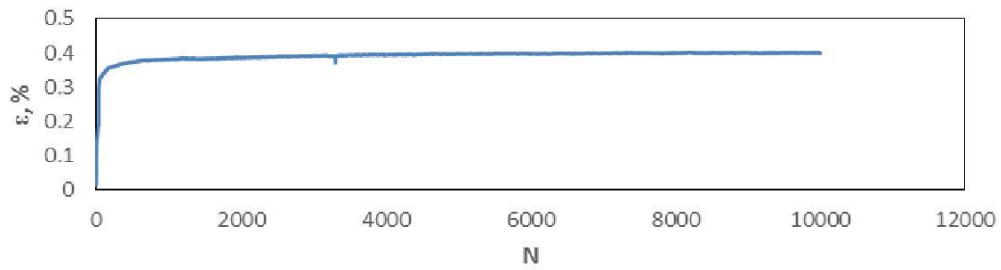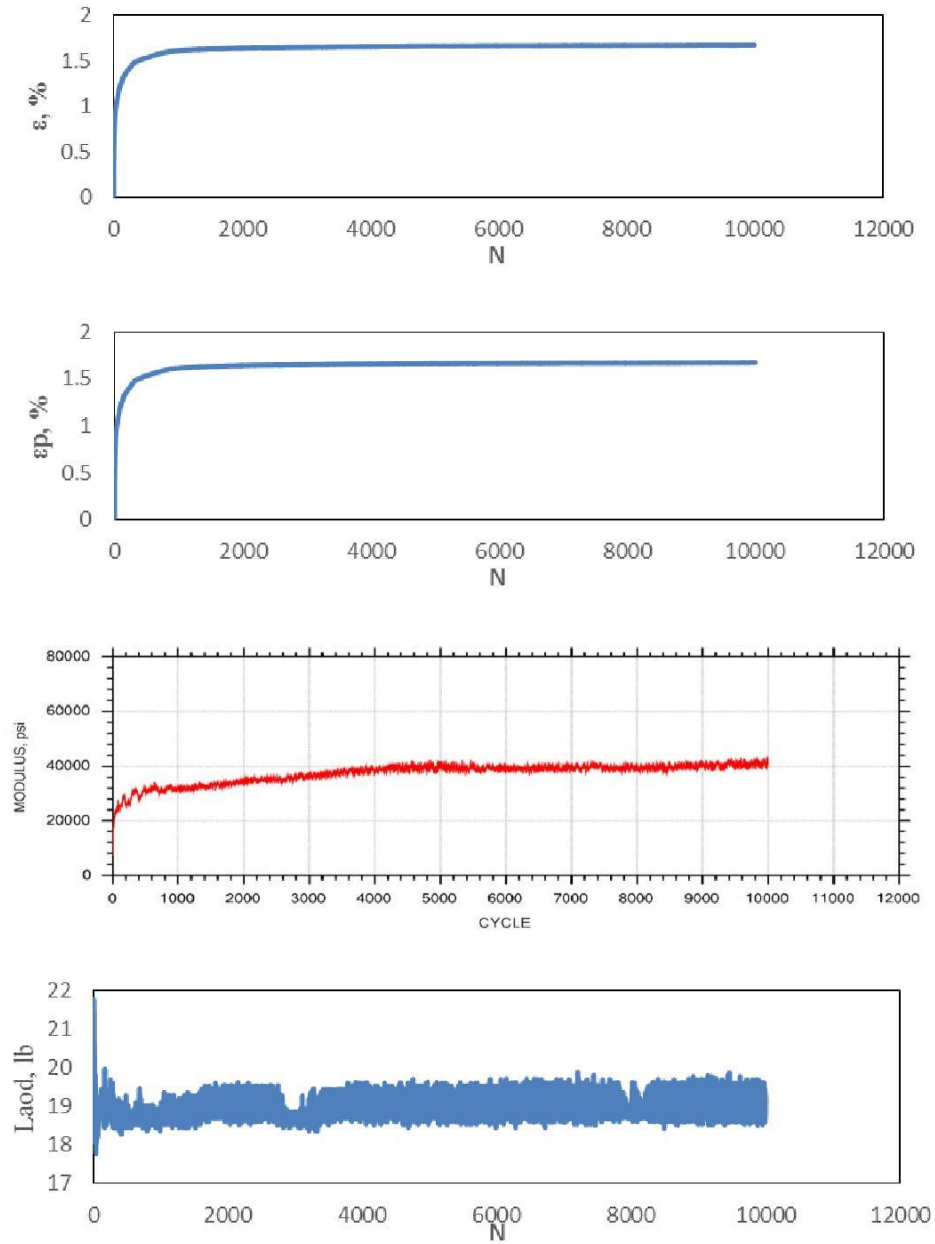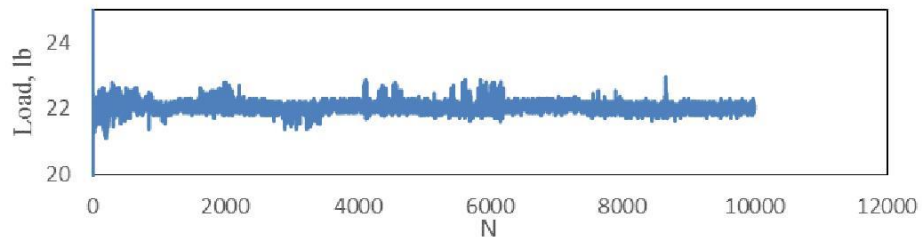| Diameter (inch)	Height (inch)	Density (g/cc)
2.84	6.13	1.59
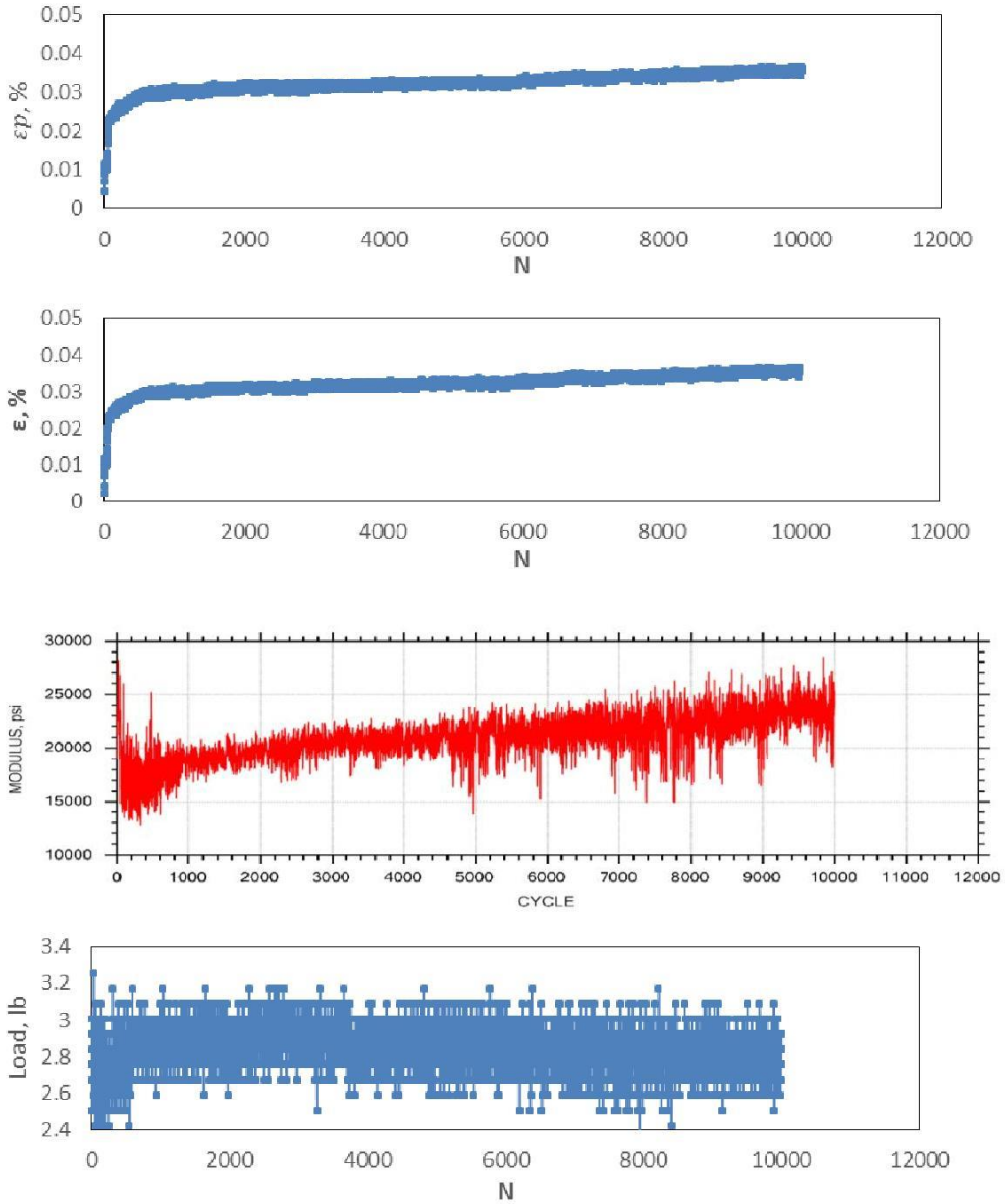
Figure A.1 Graphs with confining pressure 5 psi and deviator stress 5 psi

Confining pressure, (psi)	Deviator Stress, (psi)	Contact pressure (psi)	Number of loading cycles, N
5	10	1	10,000

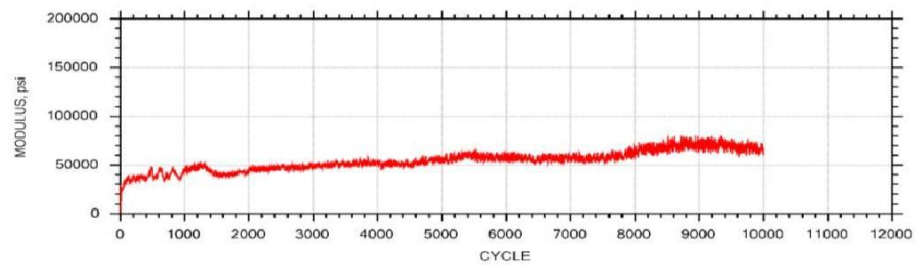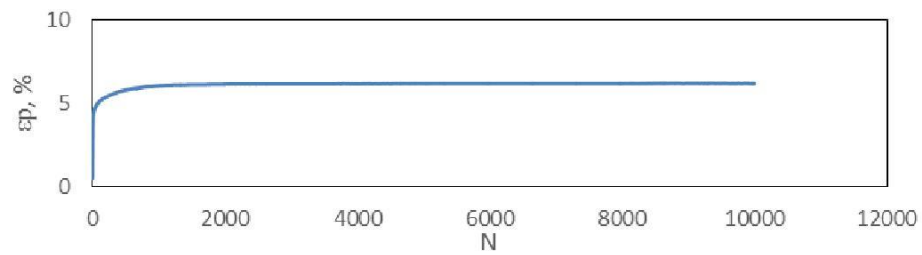| Diameter (inch)	Height (inch)	Density (g/cc)
2.84	6.13	1.58
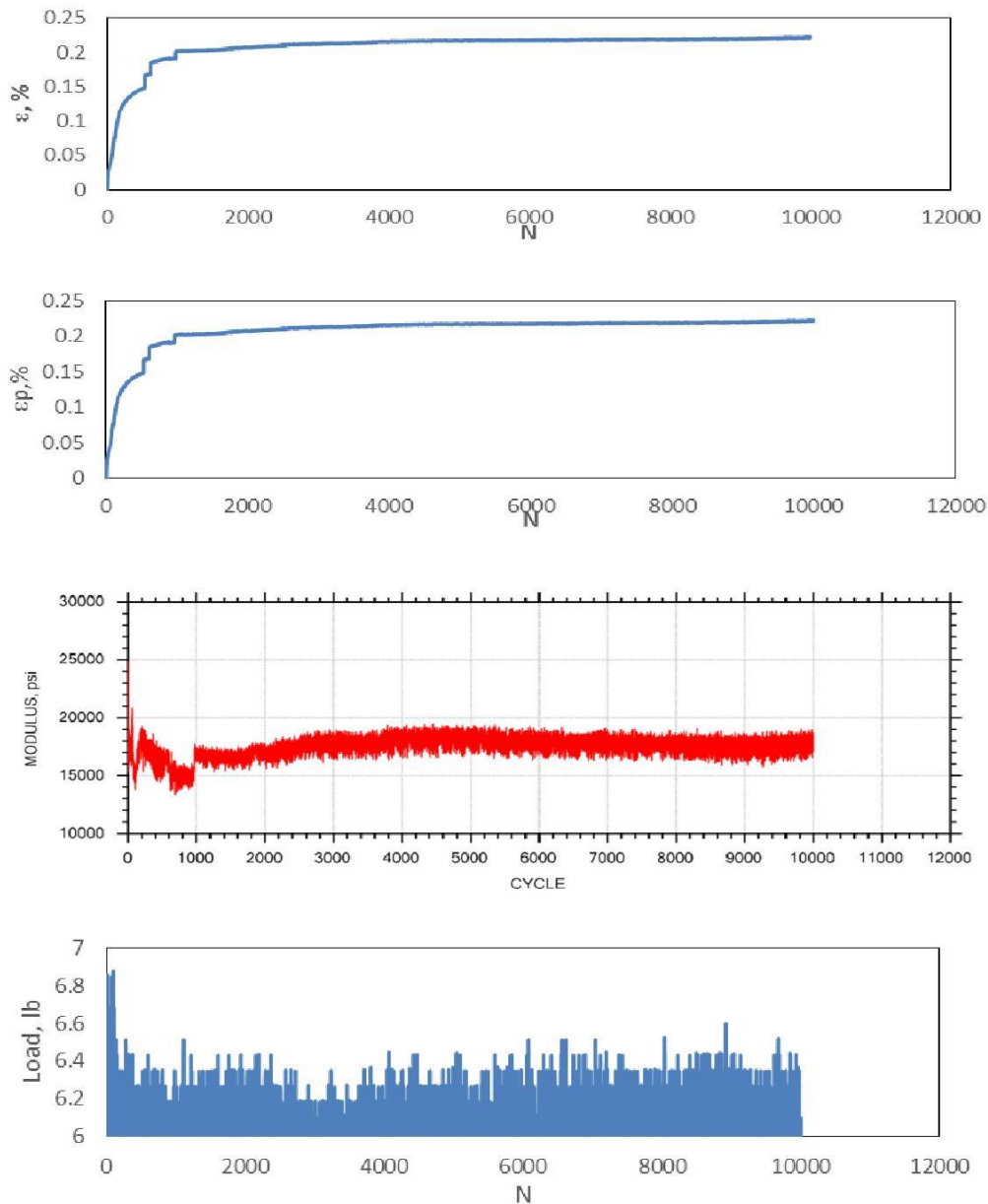
Figure A.2 Graphs with confining pressure 5 psi and deviator stress 10 psi

Confining pressure, (psi)	Deviator Stress, (psi)	Contact pressure (psi)	Number of loading cycles, N
5	15	1.5	10,000

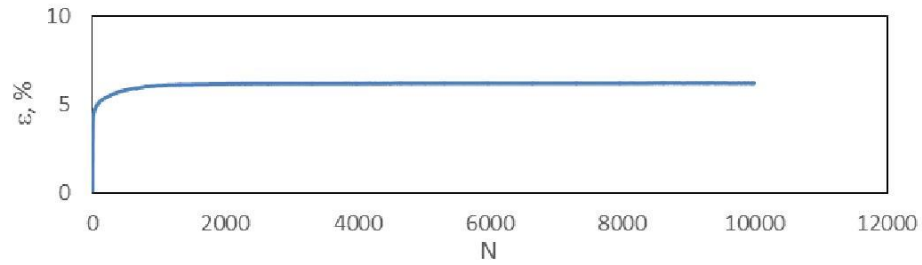| Diameter (inch)	Height (inch)	Density (g/cc)
2.84	6.05	1.57
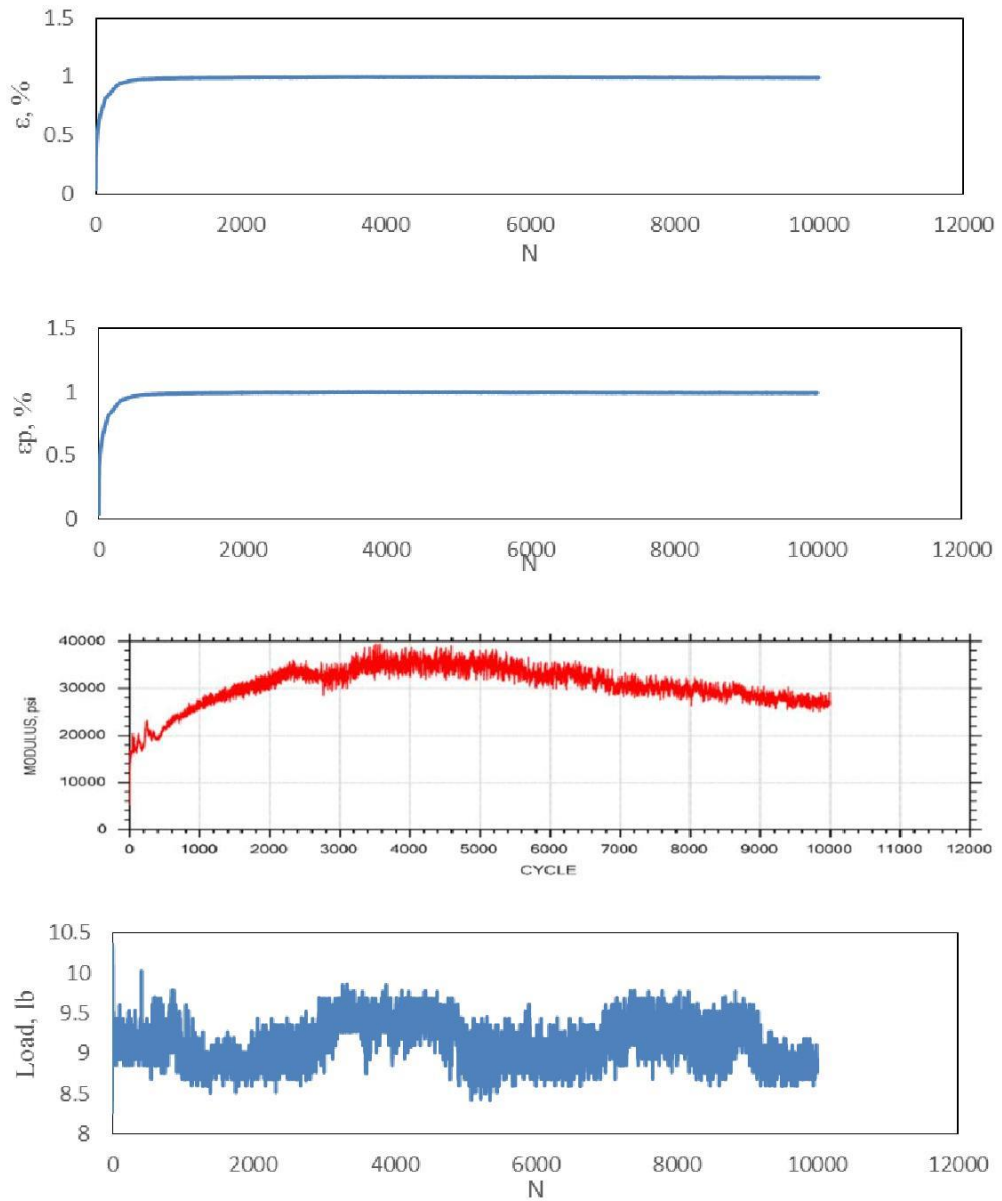
Figure A.3 Graphs with confining pressure 5 psi and deviator stress 15 psi

Confining pressure, (psi)	Deviator Stress, (psi)	Contact pressure (psi)	Number of loading cycles, N
5	20	2	10,000

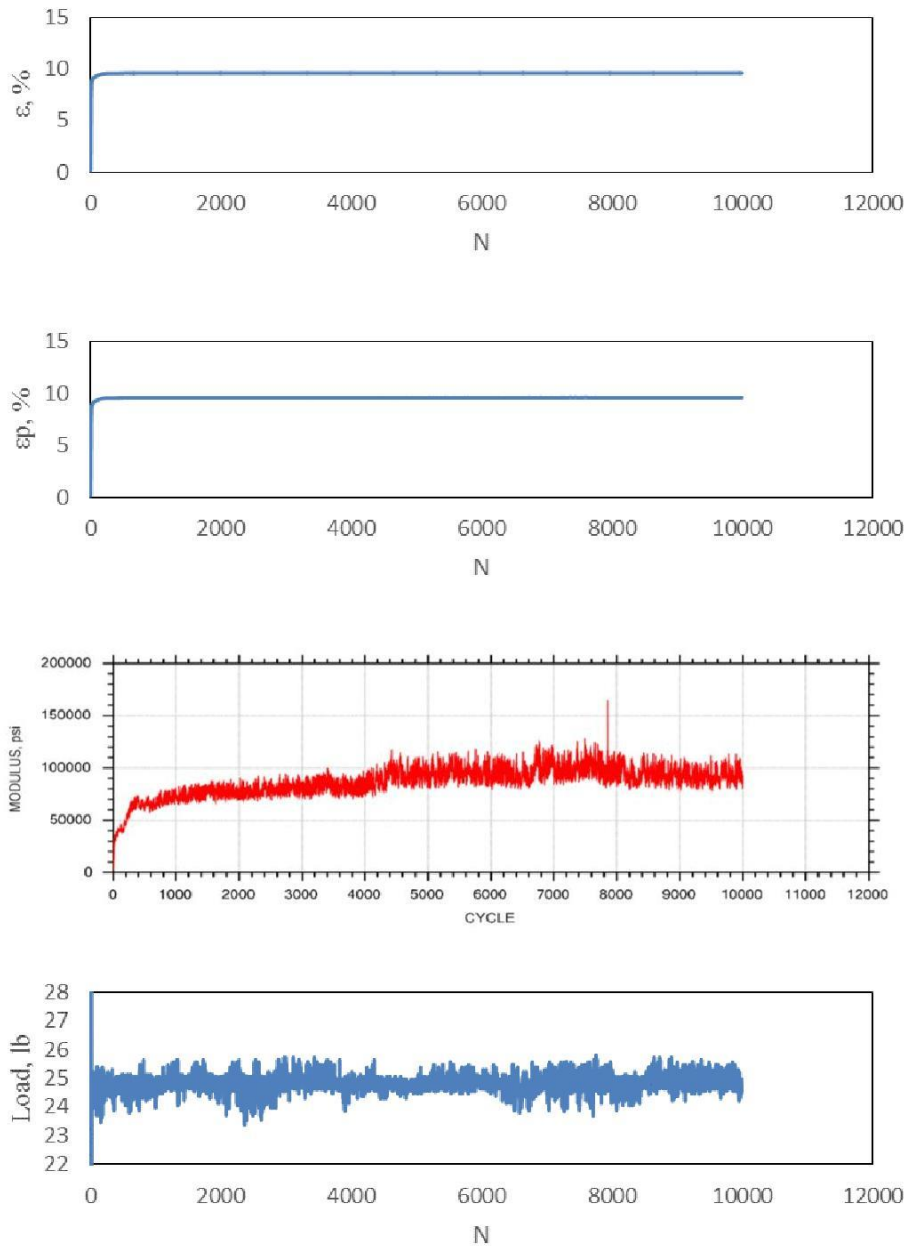| Diameter (inch)	Height (inch)	Density (g/cc)
2.84	6.10	1.58
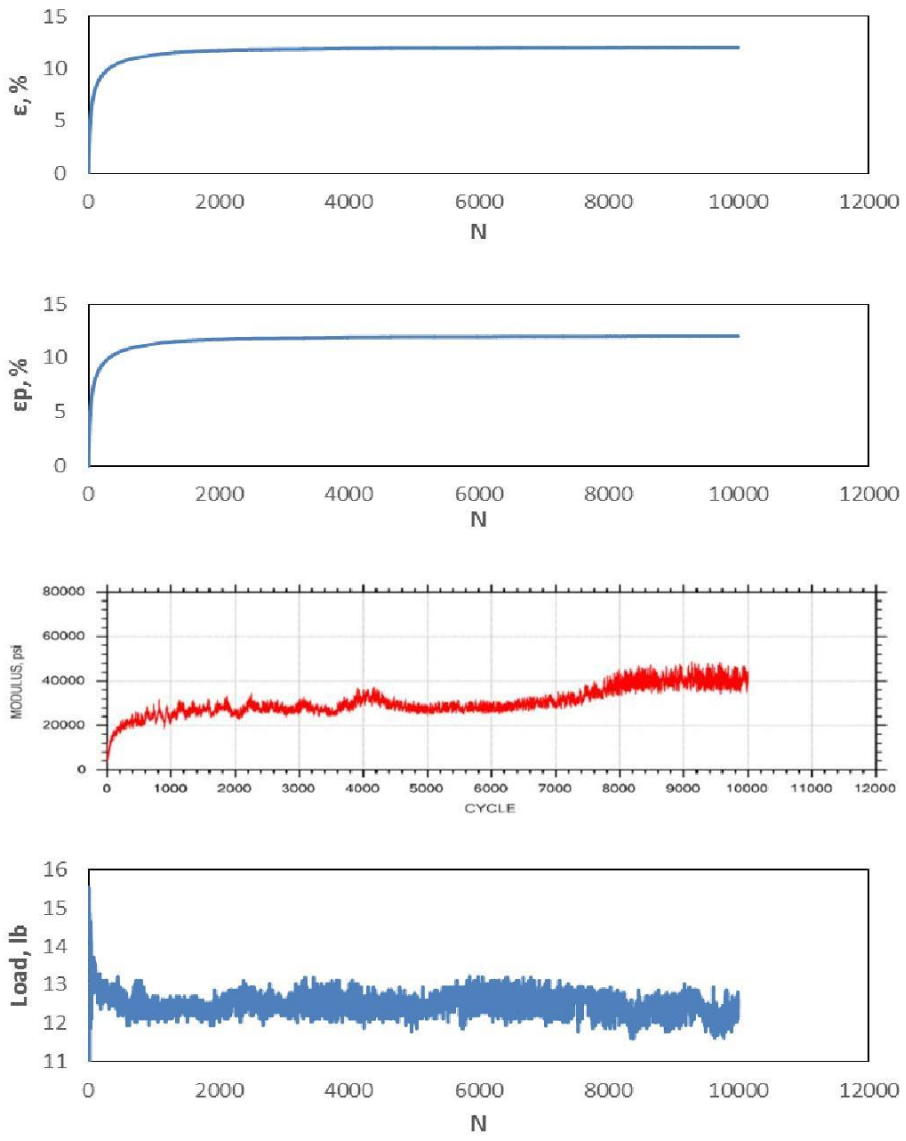
Figure A.4 Graphs with confining pressure 5 psi and deviator stress 20 psi

Confining pressure, (psi)	Deviator Stress, (psi)	Contact pressure (psi)	Number of loading cycles, N
10	10	1	10,000

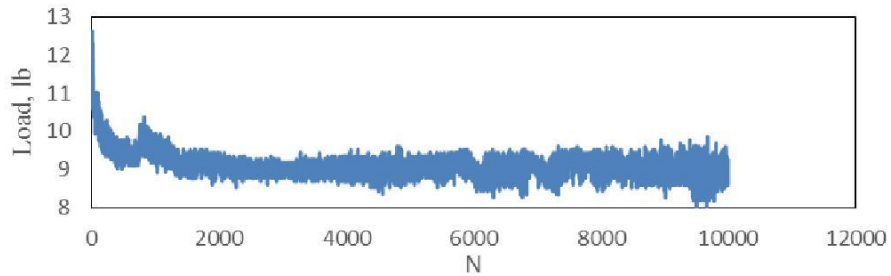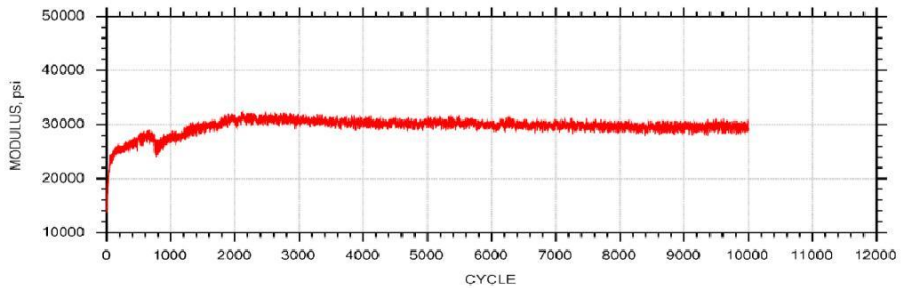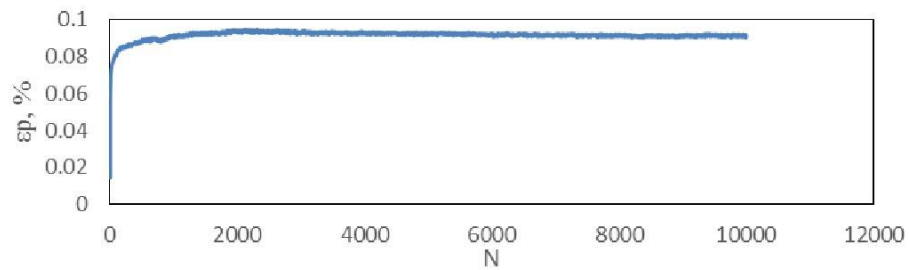| Diameter (inch)	Height (inch)	Density (g/cc)
2.84	6.10	1.59
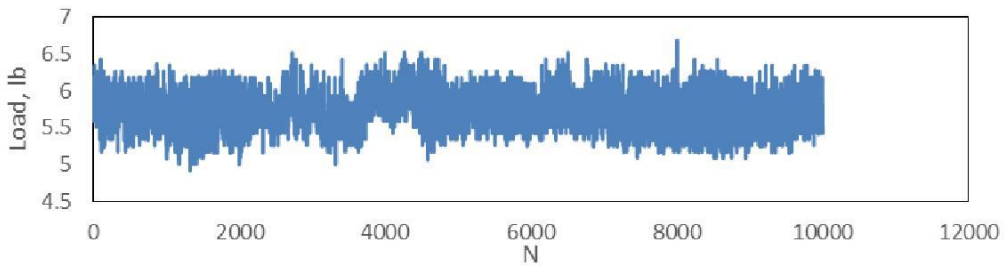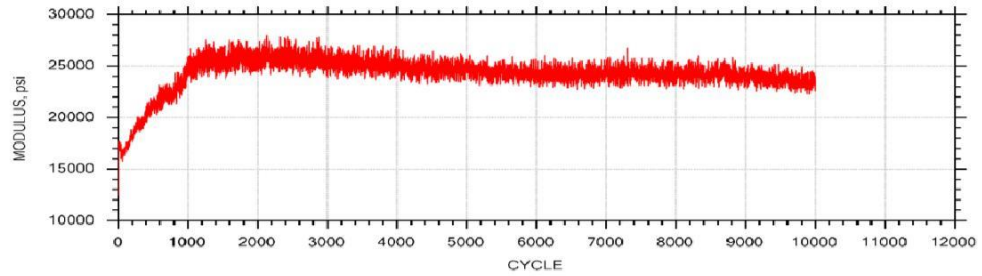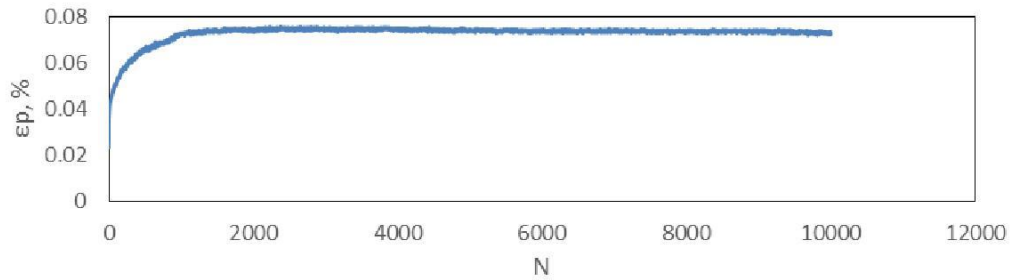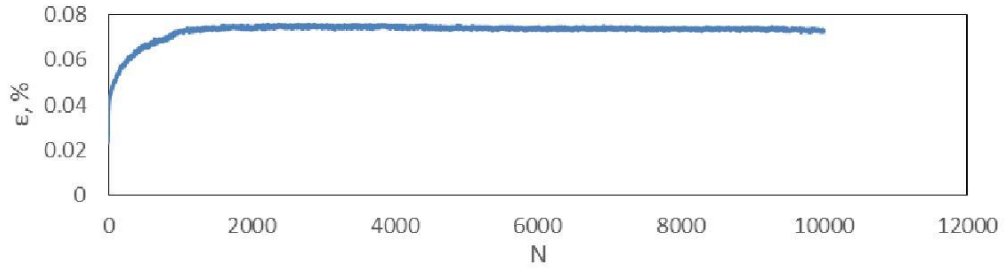
Figure A.5 Graphs with confining pressure 10 psi and deviator stress 10 psi

Confining pressure, (psi)	Deviator Stress, (psi)	Contact pressure (psi)	Number of loading cycles, N
10	20	2	10,000

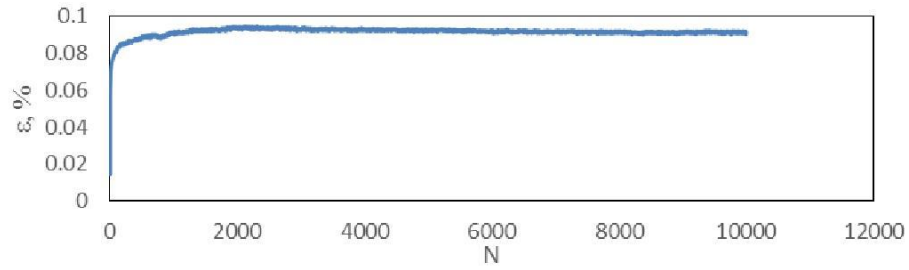| Diameter (inch)	Height (inch)	Density (g/cc)
2.84	6.10	1.59
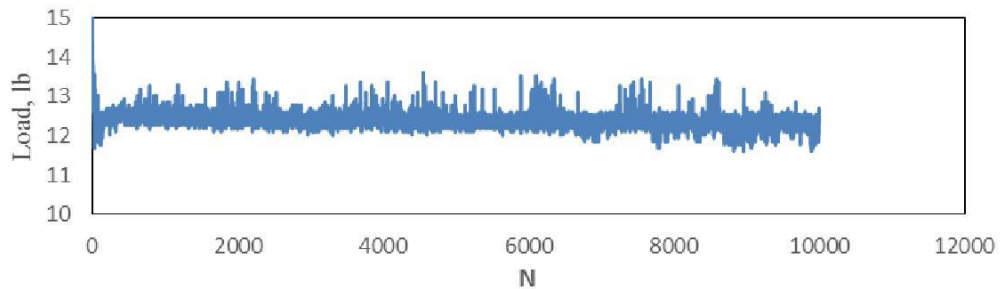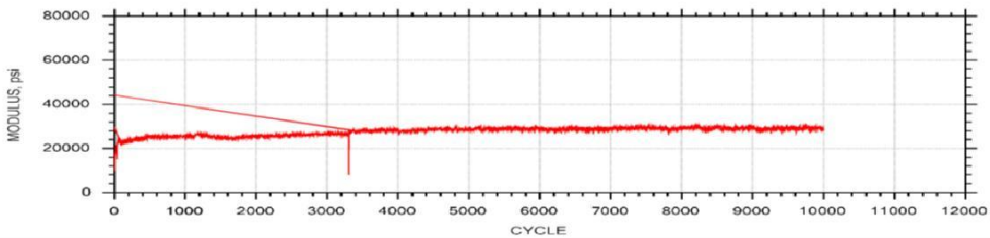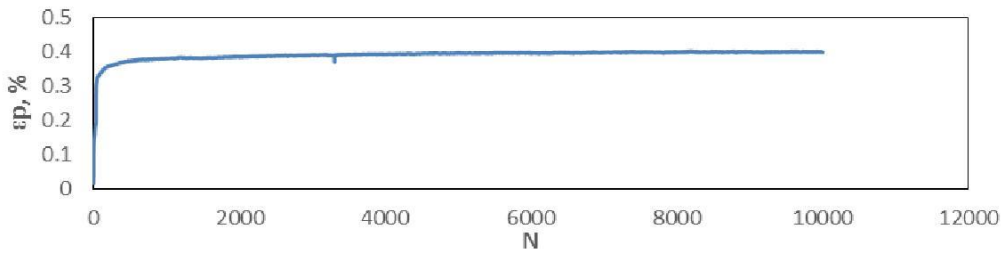
Figure A.6 Graphs with confining pressure 10 psi and deviator stress 20 psi

Confining pressure, (psi)	Deviator Stress, (psi)	Contact pressure (psi)	Number of loading cycles, N
10	30	3	10,000

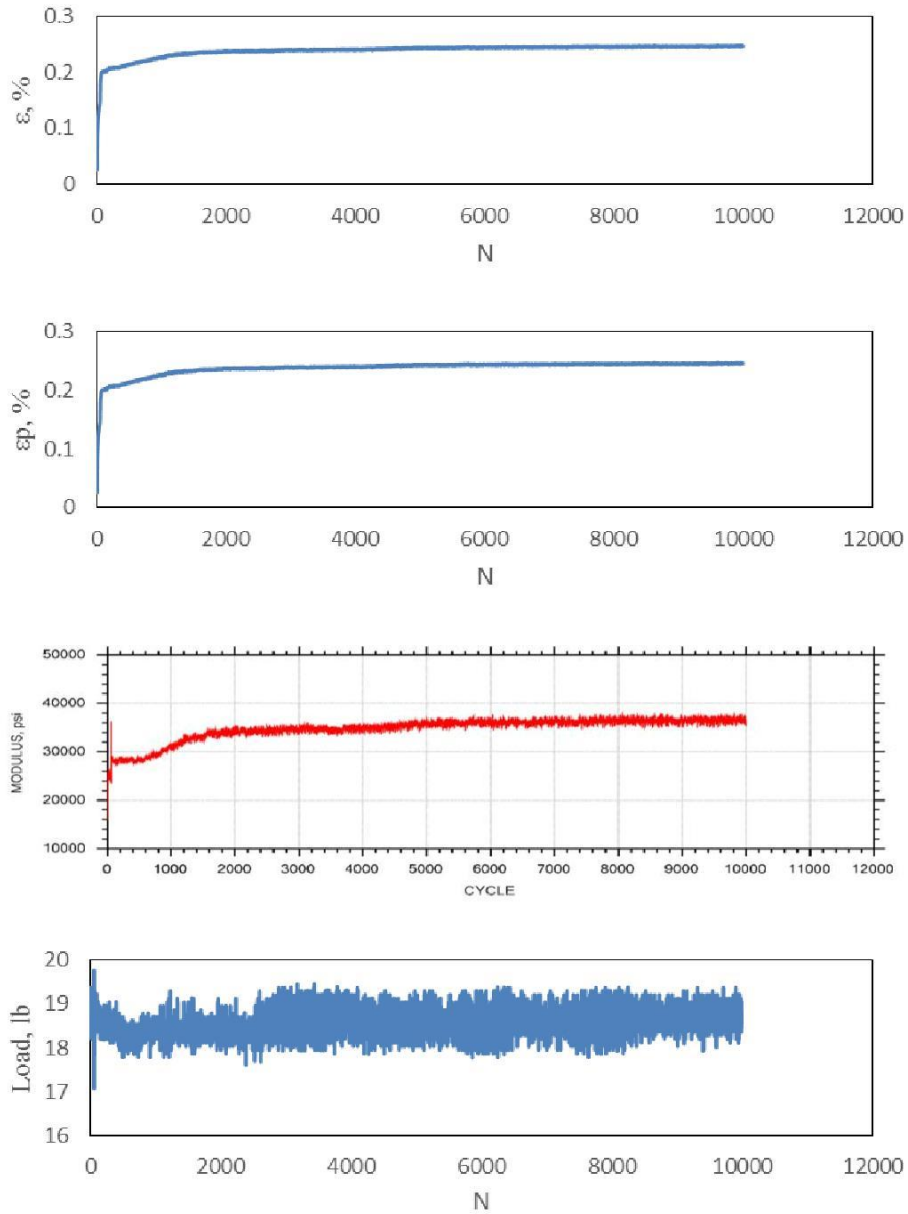| Diameter (inch)	Height (inch)	Density (g/cc)
2.84	6.10	1.56

Figure A.7 Graphs with confining pressure 10 psi and deviator stress 30 psi

Confining pressure, (psi)	Deviator Stress, (psi)	Contact pressure (psi)	Number of loading cycles, N
10	35	3.5	10,000

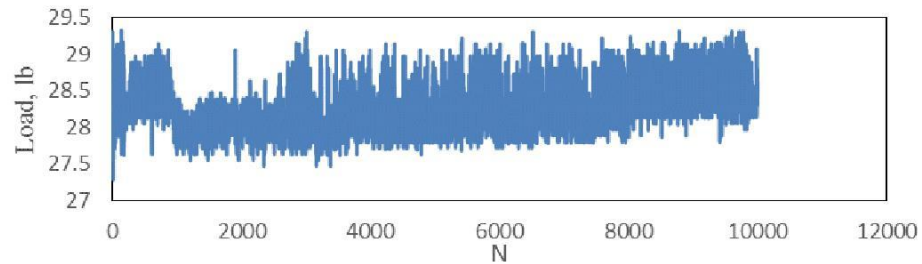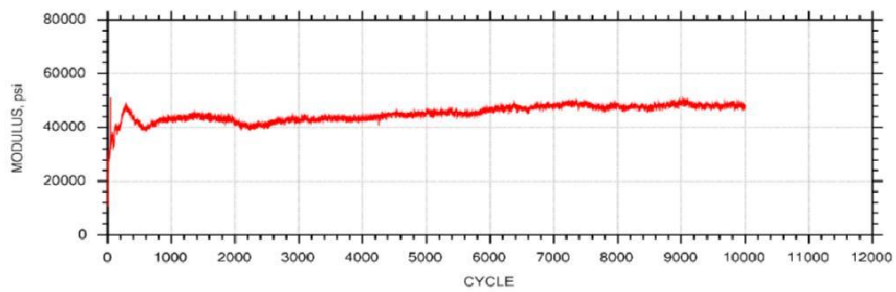| Diameter (inch)	Height (inch)	Density (g/cc)
2.84	6.12	1.57

Figure A.8 Graphs with confining pressure 10 psi and deviator stress 35 psi

Confining pressure, (psi)	Deviator Stress, (psi)	Contact pressure (psi)	Number of loading cycles, N
10	40	4	10,000

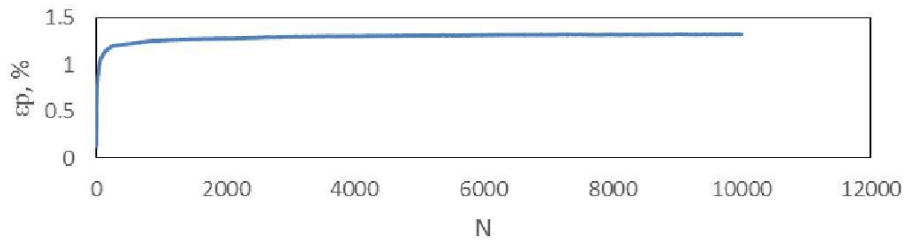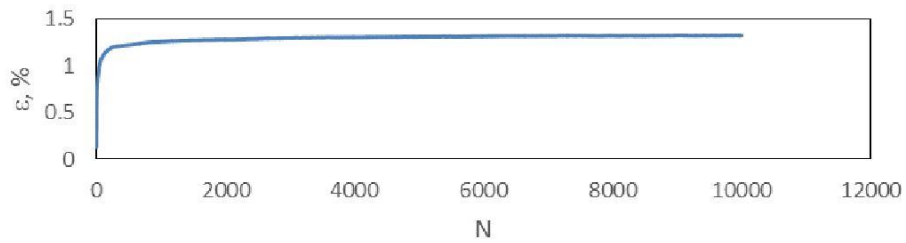| Diameter (inch)	Height (inch)	Density (g/cc)
2.85	6.13	1.58

Figure A.9 Graphs with confining pressure 10 psi and deviator stress 40 psi

Confining pressure, (psi)	Deviator Stress, (psi)	Contact pressure (psi)	Number of loading cycles, N
15	15	1.5	10,000

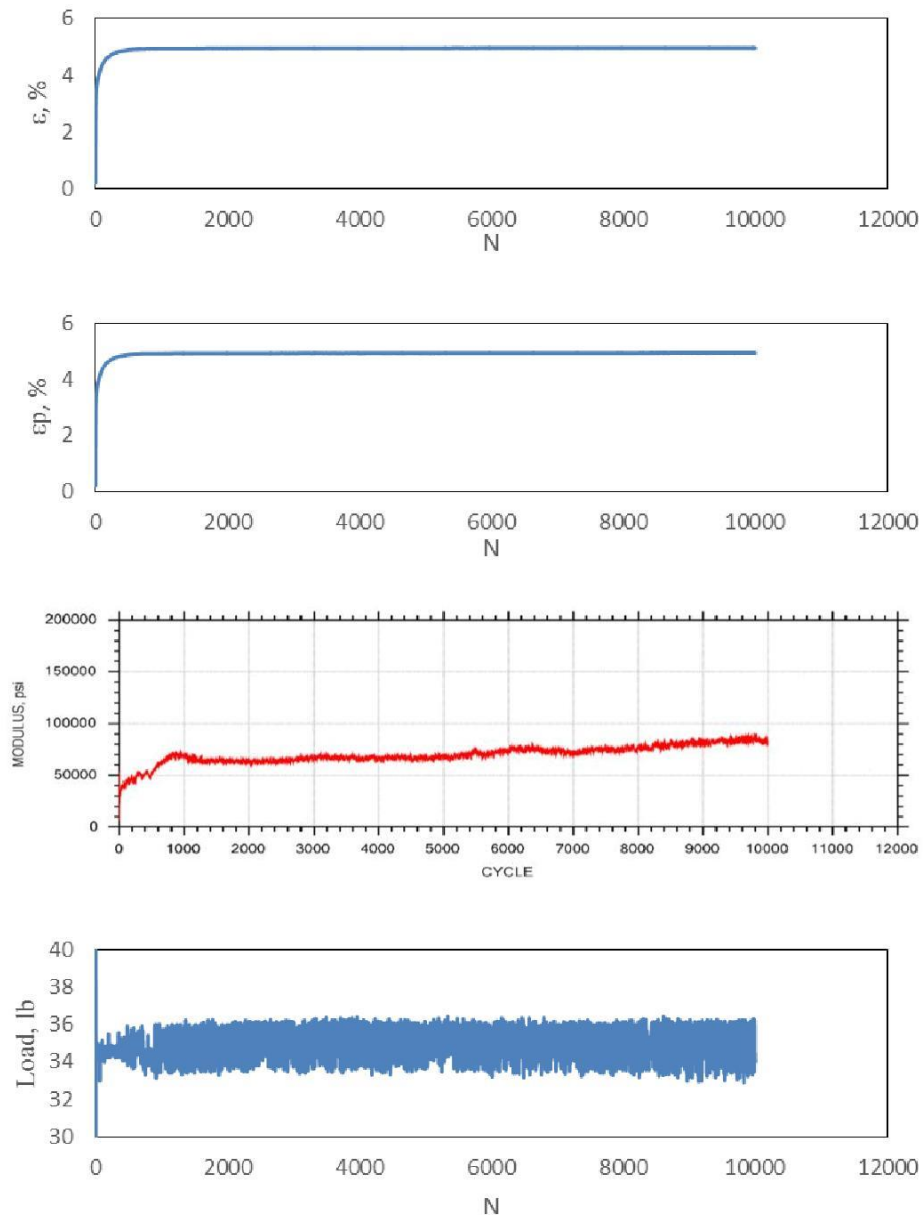| Diameter (inch)	Height (inch)	Density (g/cc)
2.84	6.10	1.58

Figure A.10 Graphs with confining pressure 15 psi and deviator stress 15 psi

Confining pressure, (psi)	Deviator Stress, (psi)	Contact pressure (psi)	Number of loading cycles, N
15	30	3	10,000

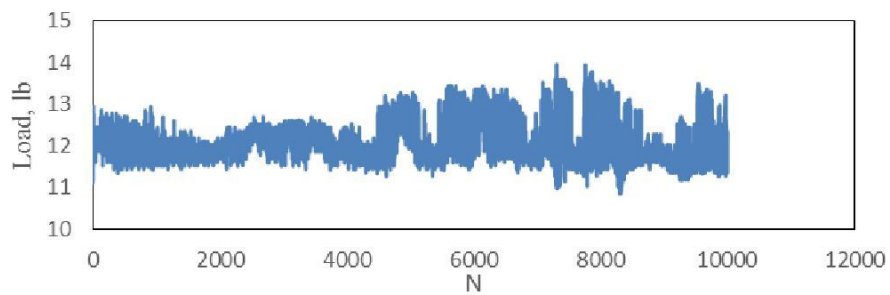| Diameter (inch)	Height (inch)	Density (g/cc)
2.84	6.10	1.60

Figure A.11 Graphs with confining pressure 15 psi and deviator stress 30 psi

Confining pressure, (psi)	Deviator Stress, (psi)	Contact pressure (psi)	Number of loading cycles, N
15	45	4.5	10,000

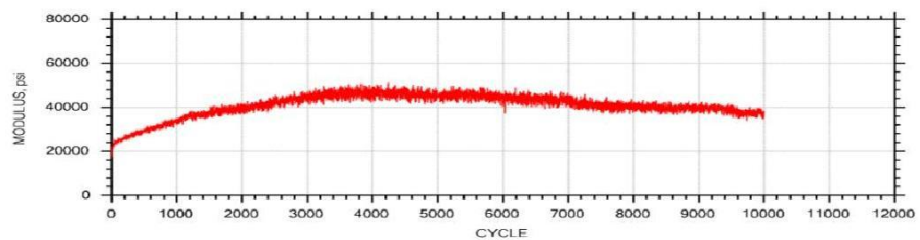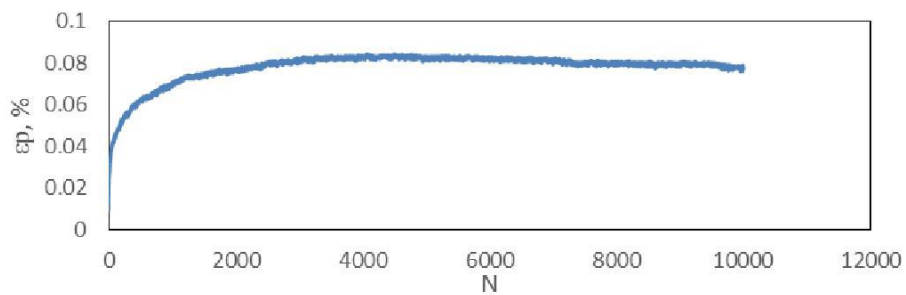| Diameter (inch)	Height (inch)	Density (g/cc)
2.84	6.08	1.59

Figure A.12 Graphs with confining pressure 15 psi and deviator stress 45 psi

Confining pressure, (psi)	Deviator Stress, (psi)	Contact pressure (psi)	Number of loading cycles, N
15	50	5	10,000

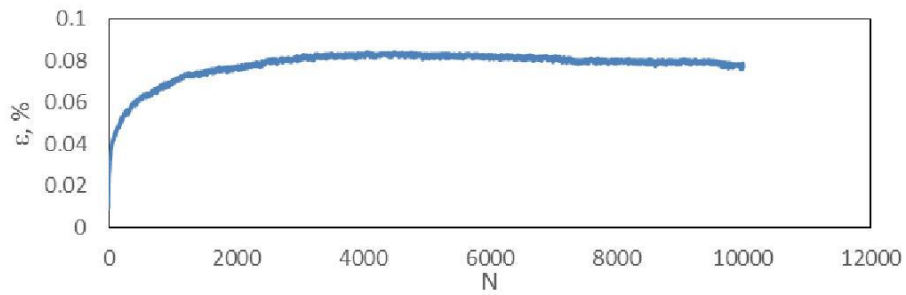| Diameter (inch)	Height (inch)	Density (g/cc)
2.84	6.19	1.59

Figure A.13 Graphs with confining pressure 15 psi and deviator stress 50 psi

Confining pressure, (psi)	Deviator Stress, (psi)	Contact pressure (psi)	Number of loading cycles, N
20	20	2	10,000

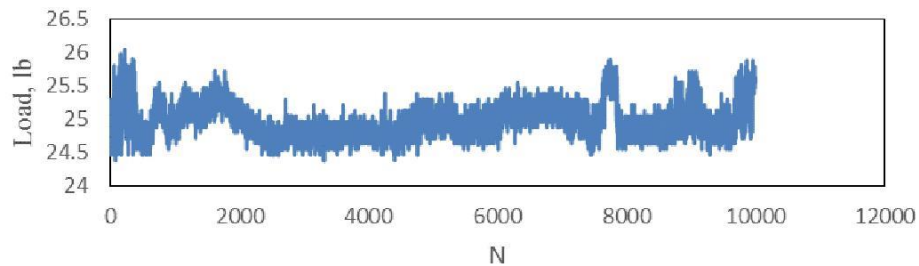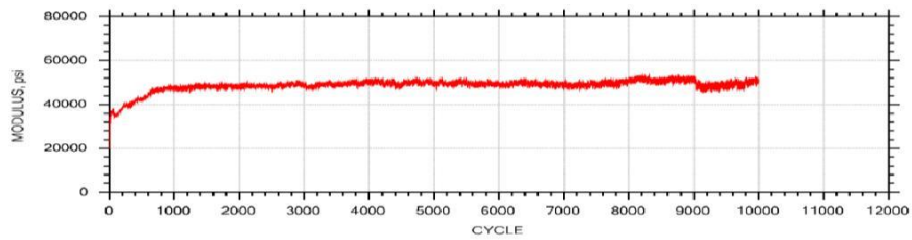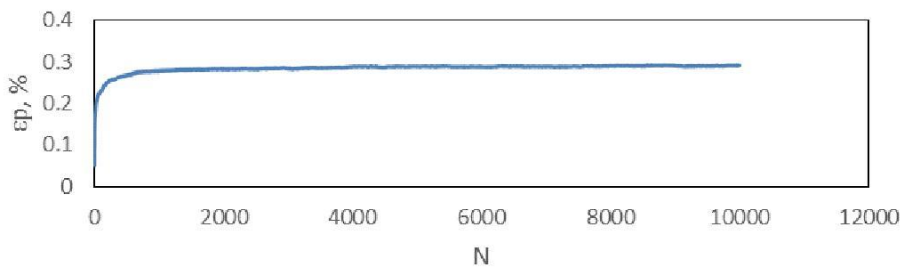| Diameter (inch)	Height (inch)	Density (g/cc)
2.84	6.12	1.59

Figure A.14 Graphs with confining pressure 20 psi and deviator stress 20 psi

Confining pressure, (psi)	Deviator Stress, (psi)	Contact pressure (psi)	Number of loading cycles, N
20	40	4	10,000

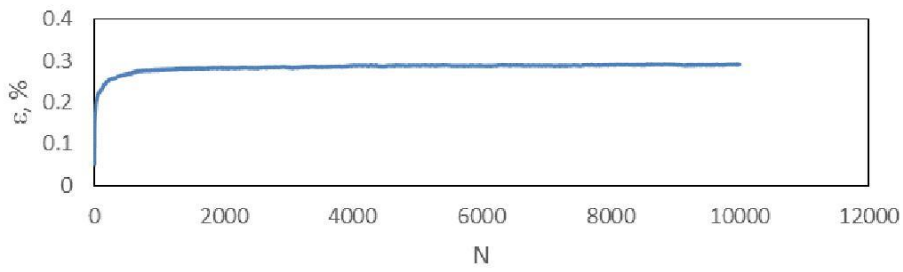| Diameter (inch)	Height (inch)	Density (g/cc)
2.85	6.14	1.58

Figure A.15 Graphs with confining pressure 20 psi and deviator stress 40 psi

Confining pressure, (psi)	Deviator Stress, (psi)	Contact pressure (psi)	Number of loading cycles, N
20	60	6	10,000

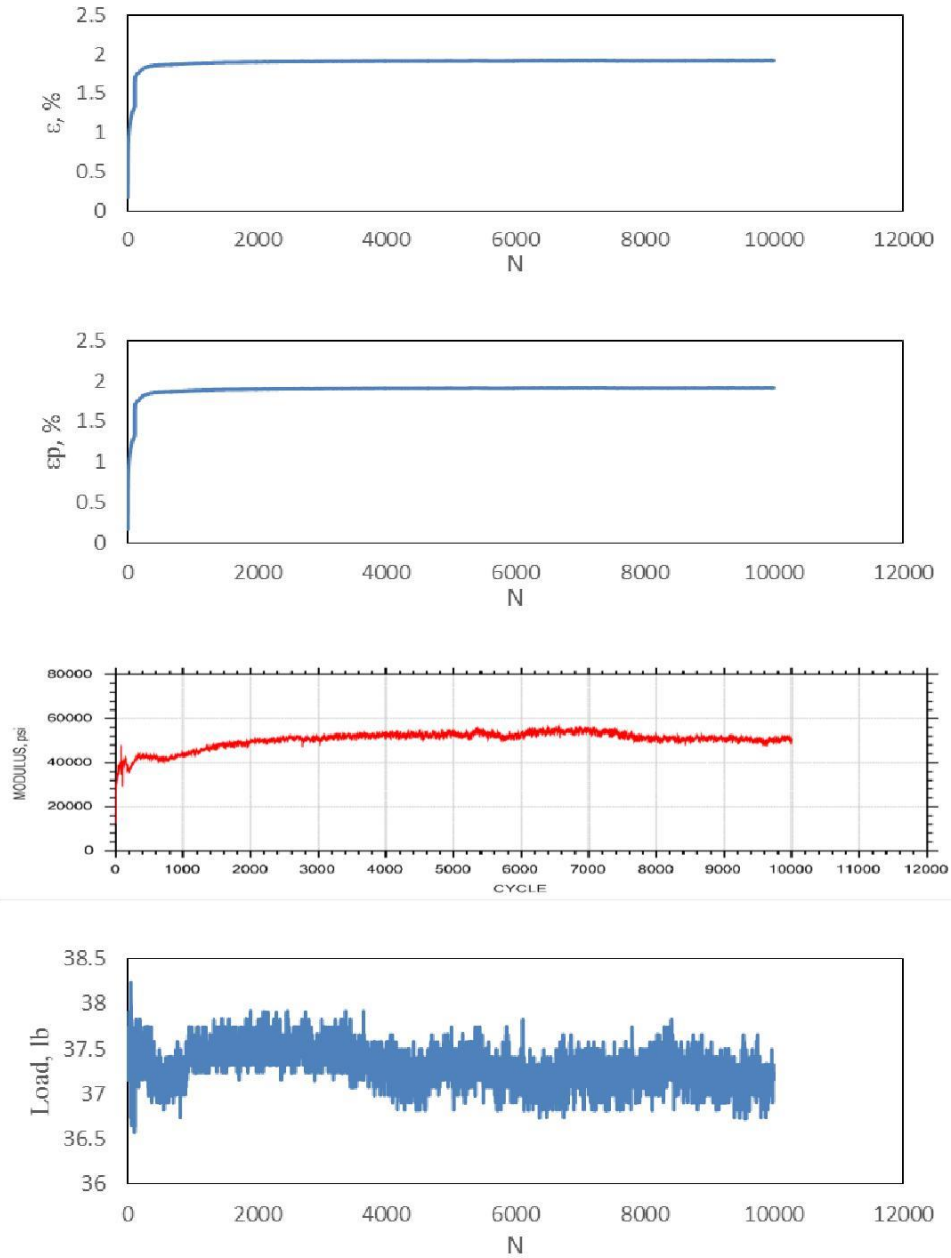| Diameter (inch)	Height (inch)	Density (g/cc)
2.83	6.09	1.59

Figure A.16 Graphs with confining pressure 20 psi and deviator stress 60 psi

Confining pressure, (psi)	Deviator Stress, (psi)	Contact pressure (psi)	Number of loading cycles, N
20	65	6.5	10,000

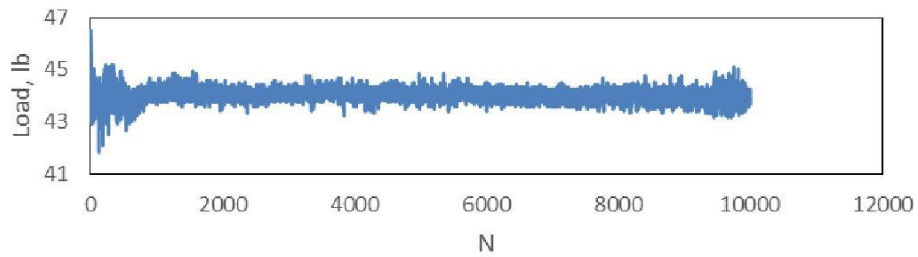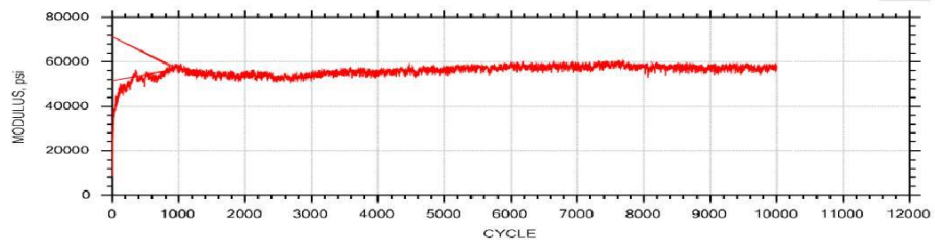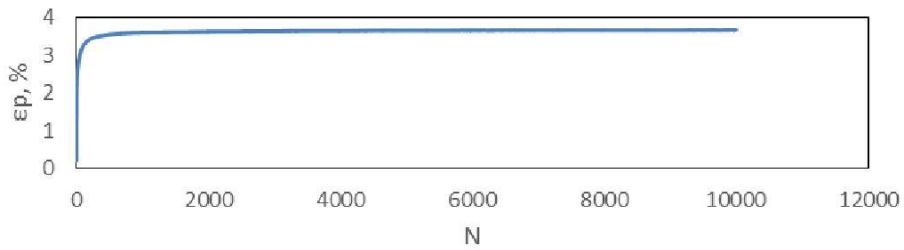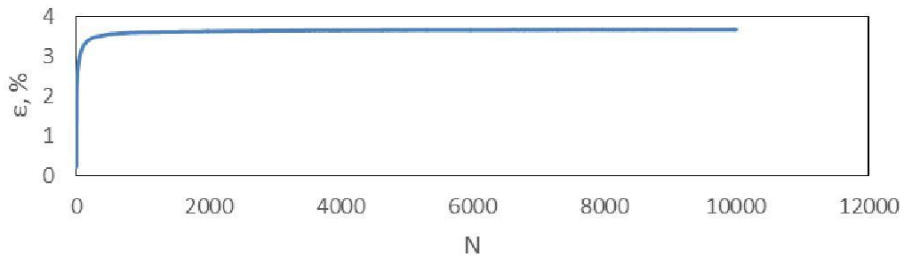| Diameter (inch)	Height (inch)	Density (g/cc)
2.84	6.05	1.60

Figure A.17 Graphs with confining pressure 20 psi and deviator stress 65 psi

B RESILIENT MODULUS TEST DATA

Confining Stress	Deviatory stress	Measured M_r
3.16	2.70	112,501.64
3.16	5.17	79,310.31
3.11	7.91	84,040.11
5.10	4.50	119,155.07
5.05	8.67	91,844.96
5.10	13.15	111,350.21
10.03	8.55	131,820.73
10.00	17.57	166,149.69
10.01	25.81	199,506.49
15.04	8.54	151,022.60
15.06	13.35	175,030.12
15.05	26.11	237,565.51
20.04	13.21	161,909.41
19.99	18.25	209,903.77
19.98	32.68	405,556.09

Figure B.1 Resilient modulus graph

k_1, k_2, k_3 are the regression co-efficients.

Atmospheric pressure = 14.7 psi

Multiple linear regression was performed to calculate the regression co-efficients.

K_1	K_2	K_3	R^2
809.379	0.318	1.060	0.81

SPANDANA ANNAMRAJU

Candidate for the Degree of

Master of Science

Thesis: Experimental and statistical study on the permanent deformation behavior of

granular soil

Major Field: Civil Engineering

Biographical:

Education:

Completed the requirements for the Master of Science in Civil and
Environmental Engineering at Oklahoma State University, Stillwater, Oklahoma
in December, 2014.

Completed the requirements for the Bachelor of Technology in Civil
Engineering at Gayatri Vidya Parishad College of Engineering, Visakhapatnam,
Andhra Pradesh/India in 2011.